Semiconductor Device Simulation for CCDs Using Drift-diffusion and Hydrodynamic Formulations

John R. F. McMacken and Savvas G. Chamberlain
Electrical and Computer Engineering Department
University of Waterloo
Waterloo, Ontario, Canada
Phone:(519)-884-1211x4598 FAX:(519)-746-3077

The Device Simulation Problem

A variety of structures

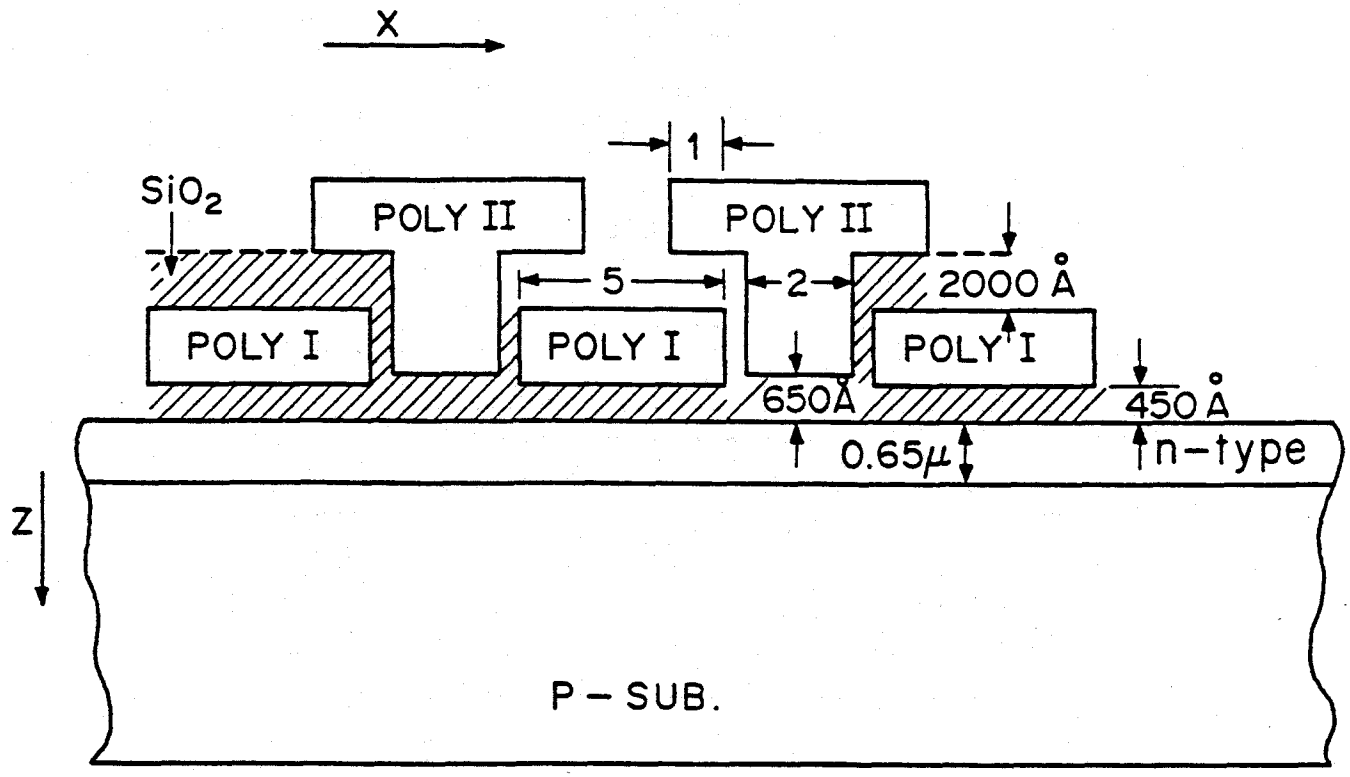

- DIMENSIONS IN μm OR AS SHOWN

Outline

The Device Simulation Problem

Carrier Transport Modeling

- Boltzmann transport equation
- energy-momentum
- drift-diffusion

Physical Property Modeling

- mobility
- recombination

Process Simulation

Discretization

Solution Methods

Examples

The Device Simulation Problem

Carrier transport modelling

$$\nabla \cdot E = \frac{q}{\epsilon}[N_D - N_A + p - n]$$

$$\frac{\partial n}{\partial t} = \frac{1}{q}\nabla \cdot J_n - R$$

$$-\frac{\partial p}{\partial t} = \frac{1}{q}\nabla \cdot J_p - R$$

$$J_n = -q\mu_n n \nabla \psi + qD_n \nabla n$$

$$J_p = -q\mu_p p \nabla \psi - qD_p \nabla p$$

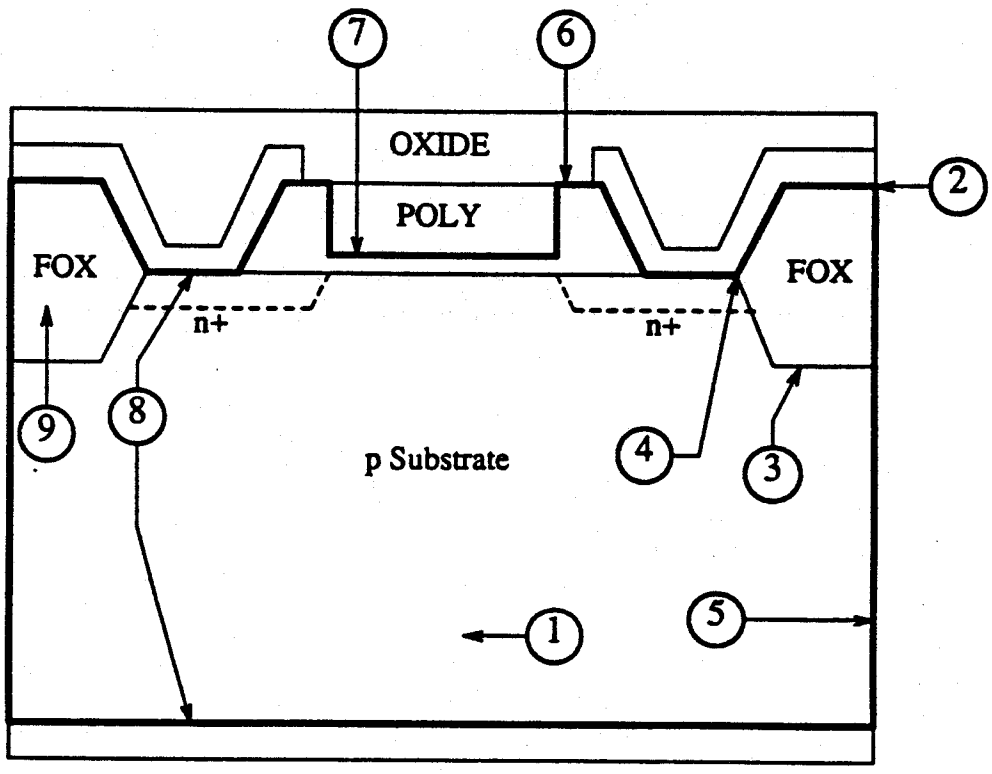

The Device Simulation Problem

A variety of structures

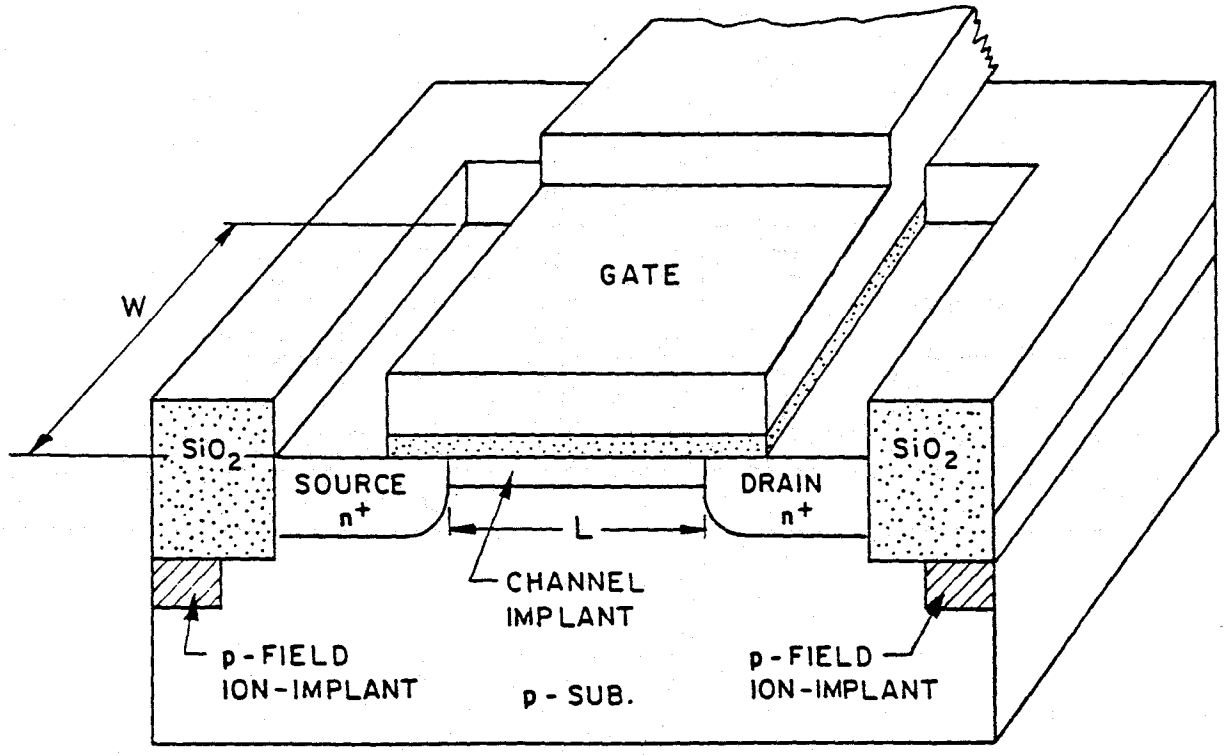

3-DIMENSIONAL N-CHANNEL MOSFET

The Device Simulation Problem

Equation solution

Finite difference or finite element discretization

- finite difference is traditional, finite element more flexible

Discretized systems may be solved using either uncoupled or fully coupled techniques

- early work used uncoupled technique
- Newton-Raphson now more popular

Either iterative or direct methods for solving linear systems

- LU decomposition
- Gauss-Sidel/Jacobi
- iterative conjugate gradient

The Device Simulation Problem

Grid generation

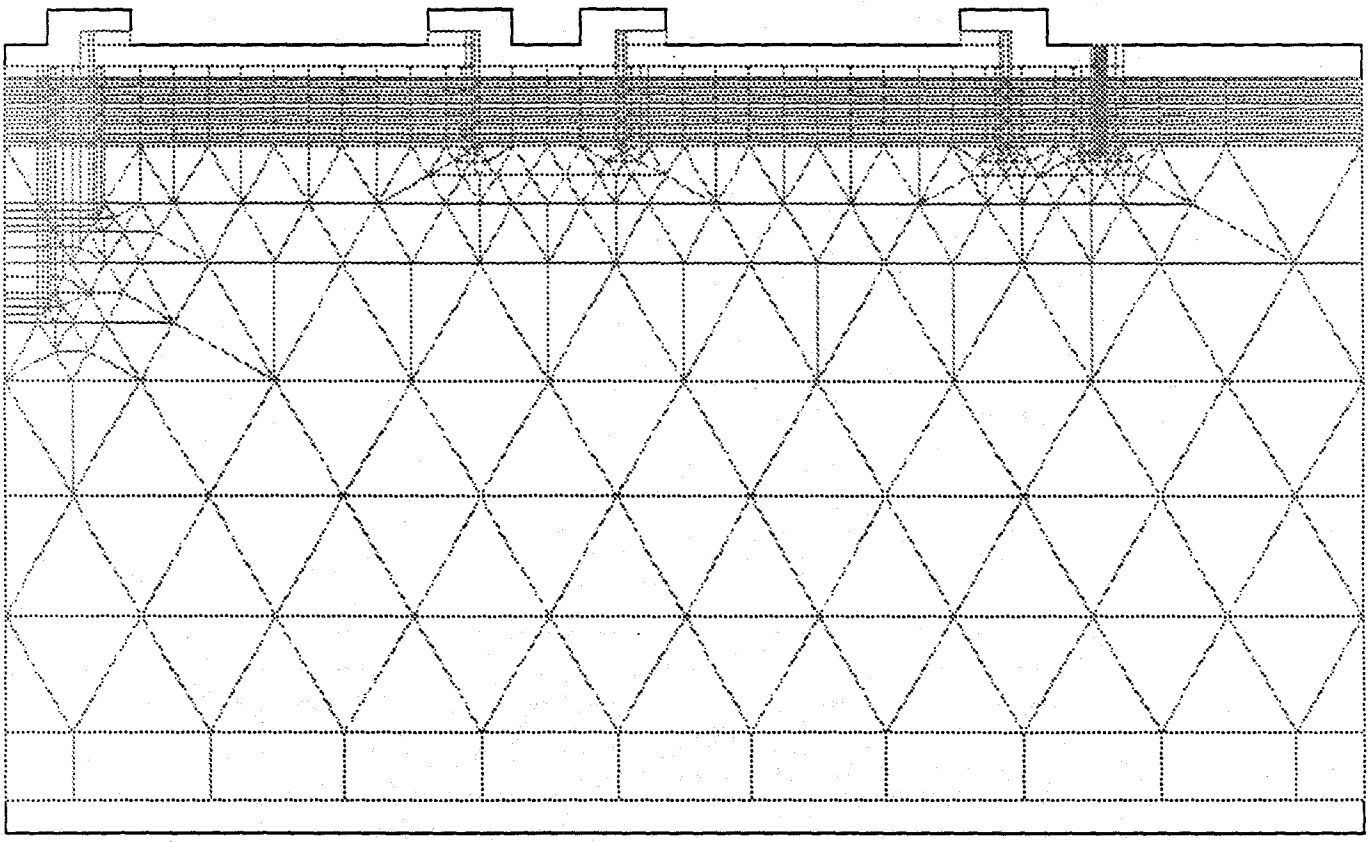

Carrier transport modelling
The Boltzmann transport equation

Most semiconductor models are based on the Boltzmann transport equation

$$\left(\frac{df}{dt}\right)_{scat} = \frac{\partial f}{\partial t} + v \cdot \nabla_r f + \frac{dk}{dt} \cdot \nabla_k f$$

The BTE describes the motion of a particle under an external force through seven-dimensional *phase space*

- three spatial coordinates (r), three momentum coordinates (k) and time

$f(k, r, t)$ is a distribution function over phase space defined such that

$$\frac{1}{4\pi^3} f(k, r, t) dk dr$$

gives the number of carriers at time t within a volume dr with momentum near dk

The Device Simulation Problem

Data analysis

- calculation of terminal currents
- regions of high electric fields
- quantum efficiency
- spectral response
- transit time
- potential distributions
- charge transfer efficiency

Carrier transport modelling
The Boltzmann transport equation

Under and electric field, a carrier is accelerated in free flight

Free flight is interrupted by a series of scattering events (collisions)

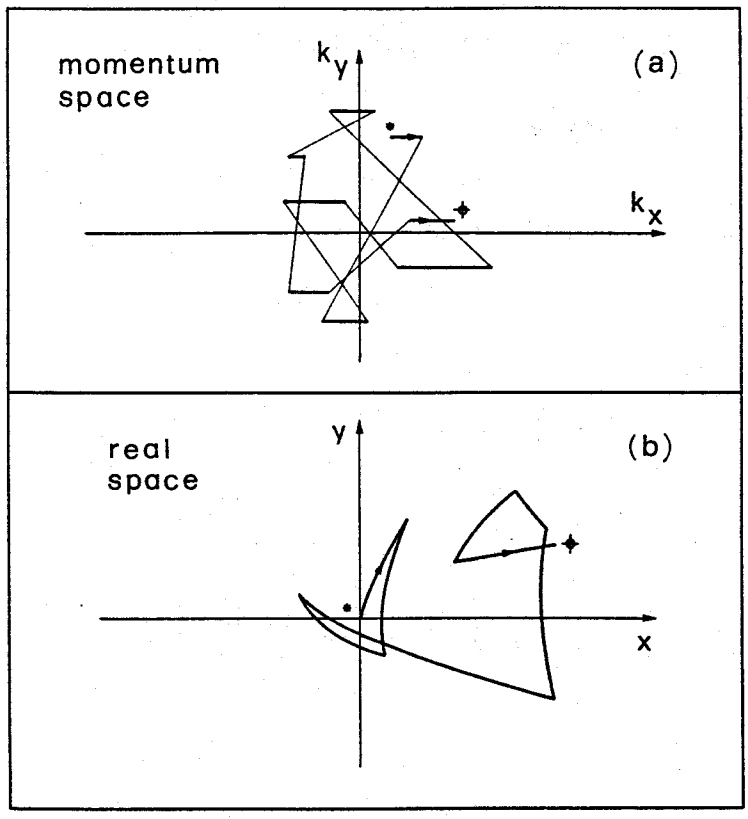

from Jacoboni and Lugli, "The Monte Carlo Method for Semiconductor Device Simulation", Spring-Verlag, 1989

- The BTE is simply an expression of conservation of energy and mass over time

Carrier transport modelling
The Boltzmann transport equation

Carrier dynamics are based on the energy-band diagram

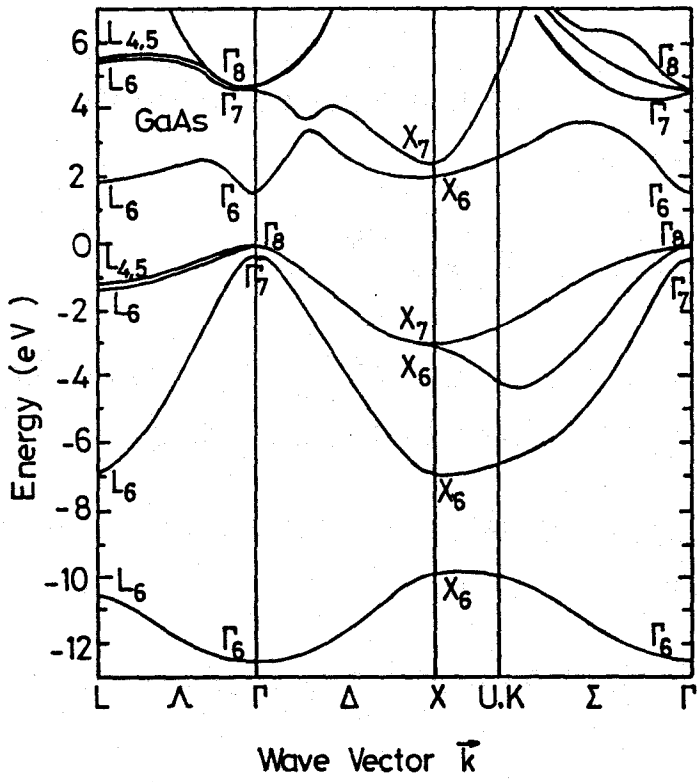

from Ridley,"Quantum Processes in Semiconductors"Oxford University Press, 1988

$$v = \frac{2\pi}{h}\nabla_k \mathcal{E} \qquad F = \frac{h}{2\pi}\frac{dk}{dt} \qquad \frac{1}{m^*_{ij}} = \left(\frac{2\pi}{h}\right)^2 \frac{\partial^2 \mathcal{E}}{\partial k_i \partial k_j}$$

Energy bands are usually simplified i.e. parabolic, isotropic

Carrier transport modelling
The Boltzmann transport equation

The BTE is based on classical gas transport and does not recognize the wave nature of the electron

Assumptions of the Boltzmann transport equation:

The effective mass theorem is valid

- external potentials vary slowly enough in space and time to prevent inter-band transistions

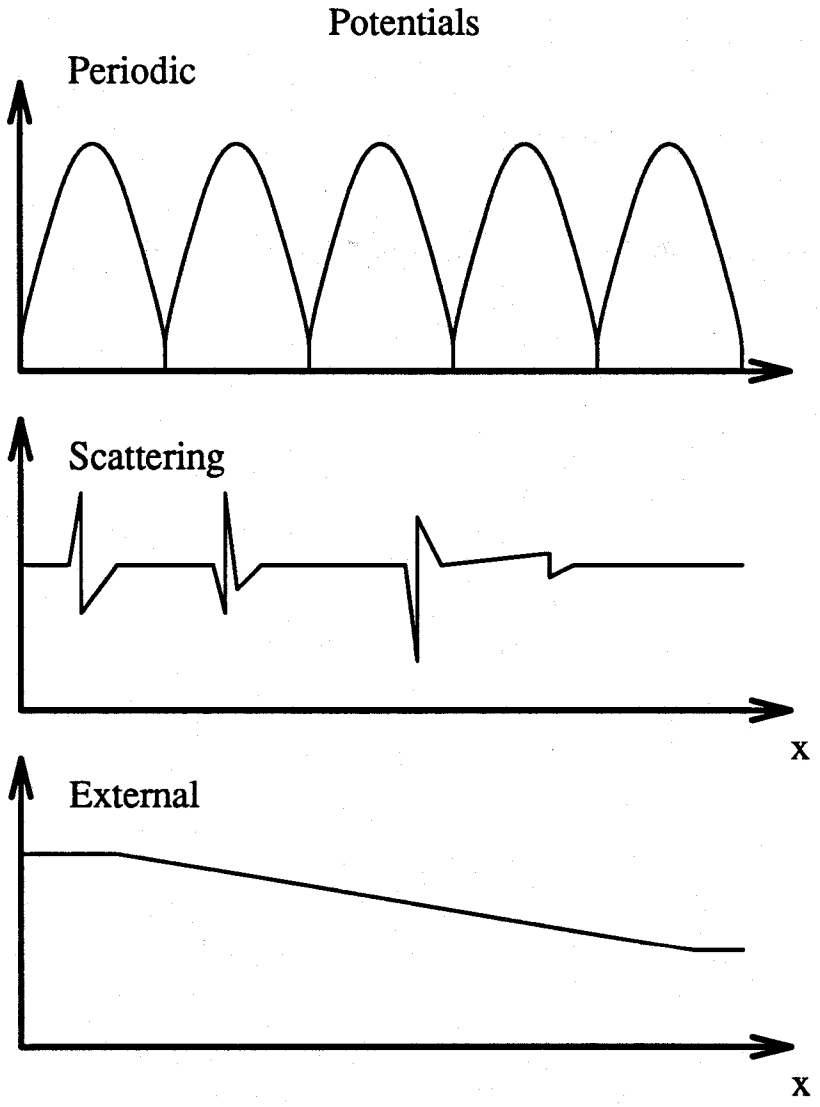

Carrier transport modelling
The Boltzmann transport equation

Analytic solutions are available only for simple cases due to the complexity of the scattering term

- statistical Monte Carlo analysis is the prefered method

Given a solution for f, we may then integrate over momentum space to determine various quantities

electron concentration

$$n(r,t) = \frac{1}{4\pi^3} \int f(k,r,t)dk$$

current

$$J(r,t)\frac{q}{4\pi^3} \int v(k)f(k,r,t)dk$$

carrier energy

$$< \mathcal{E}(r,t) >= \frac{1}{n(r,t)} \int \mathcal{E}(r,t)f(k,r,t)dk$$

Carrier transport modelling
The Boltzmann transport equation

Assumptions of the Boltzmann transport equation:

Electron wave-packets can be approximated by classical particles

Carriers must be localized within the device and fast enough to respond to the external potential

- temporal limit: given a given a wave packet with energy range $k_B T$
- from the uncertainty principle $\delta t \delta \mathcal{E} \approx h$

$$\delta t > \frac{h}{k_B T}$$

or

$$\omega << 6.3 \times 10^{12} \text{Hz}$$

Carrier transport modelling
The Boltzmann transport equation

Effective mass high frequency limit

To prevent inter-band transitions, the carrier energy $\mathcal{E}$ must be $<< \mathcal{E}_g$

- temporal limit: from $\mathcal{E} = h\omega$, we have

  $\omega << \mathcal{E}_g/h = 2.7 \times 10^{14}$Hz (Si)

- spatial limit: energy gained from falling across one atomic spacing is $\mathcal{E} = qEa$

  $$E \ll \frac{\mathcal{E}_g}{qa} = 20\text{MV/cm}$$

These are not significant limits for CCD work

Carrier transport modelling
The Boltzmann transport equation

Assumptions of the Boltzmann transport equation:

Carrier collisions are instantaneous

- collision durations are of the order of 0.03 ps
- for free-flight times of this order carriers will gain/lose significant energy during the collison

Instead of using the Monte Carlo technique to solve the BTE directly, we may assume a particular form for f and integrate over k-space

Carrier transport modelling
The Boltzmann transport equation

Assumptions of the Boltzmann transport equation:

- spatial limit:

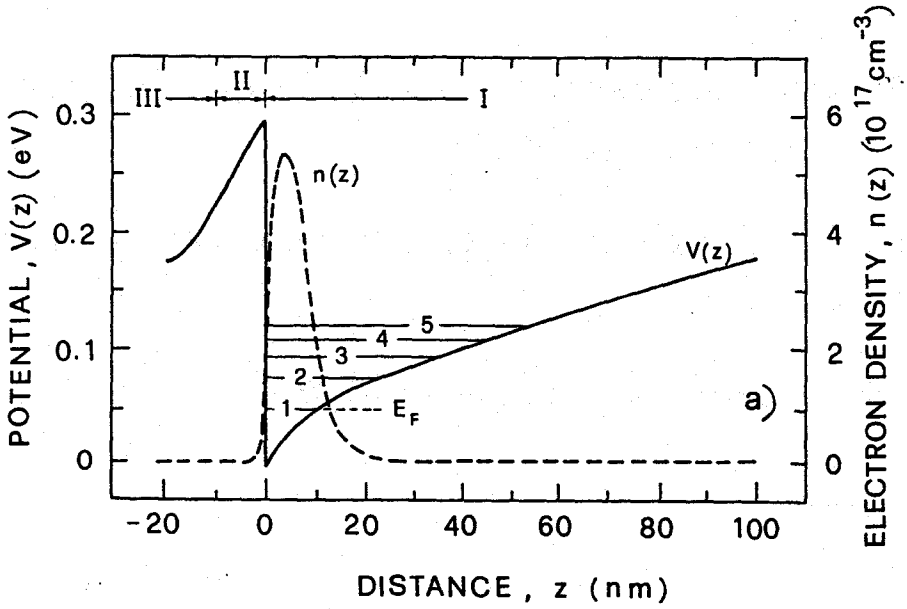

from Yokoyama and Hess, Physical Review B, 1986

- assuming a simple parabolic band with isotropic effective mass

$$k_B T = \frac{\hbar^2 \delta t k^2}{2m^*}$$

- from the uncertainty principle $\delta x \delta p \approx h$

$$\delta x \gg \frac{h}{\sqrt{2m^* k_B T}}$$

or $x \gg$ 139Ang. for silicon

Carrier transport modelling
Hydrodynamic formulation

Other assumptions:

- parabolic energy bands with spherical surfaces
  - effective mass is isotropic, independent of energy
  - reasonable assumption for low-energy carriers and 1-D current flow
- single conduction valley
  - valid for Si, problematic for GaAs
- energy and momentum restore equilibrium based on exponential decay
  - scattering is characterized by energy and momentum relaxation times

$$\left(\frac{dw_n}{dt}\right)_{scat} = n\frac{\mathcal{E} - \mathcal{E}_0}{\tau_e(\mathcal{E})} \qquad \left(\frac{dp_n}{dt}\right)_{scat} = -\frac{nm^* v_n}{\tau_m(\mathcal{E})}$$

Carrier transport modelling
Hydrodynamic formulation

If the carrier interaction is strong enough to share energy, f may be approximated by a drifted Maxwellian form:

$$f = A_0 \exp\left\{-\left[\frac{h^2(k-k_0)^2}{2m^* k_B T}\right]\right\}$$

i.e. a distribution centered at wave-vector k_0 with a characteristic temperature T

- requires carrier concentrations $\approx 10^{16} - 10^{18}\text{cm}^{-3}$
- a poor approximation for high-energy carriers

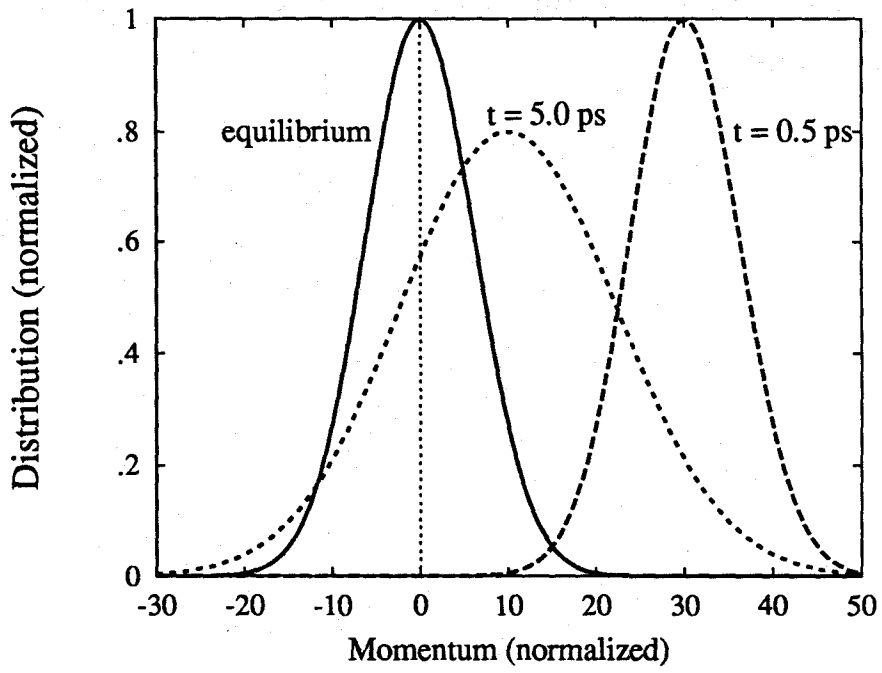

Carrier transport modelling
Hydrodynamic formulation

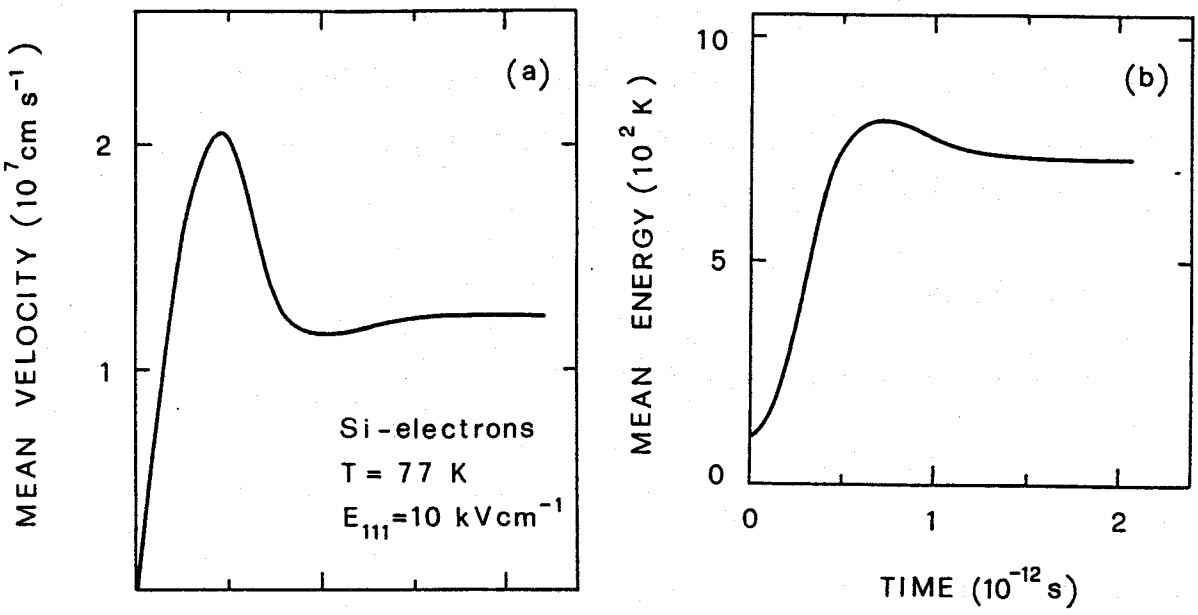

from Jacoboni and Lugli, The Monte Carlo Method for Semiconductor Device Simulation, Springer-Verlag, 1989

The difference in relaxation times leads to velocity overshoot

- in silicon, this is significant over a few tenths of a micron
- more important in GaAs

Carrier transport modelling
Hydrodynamic formulation

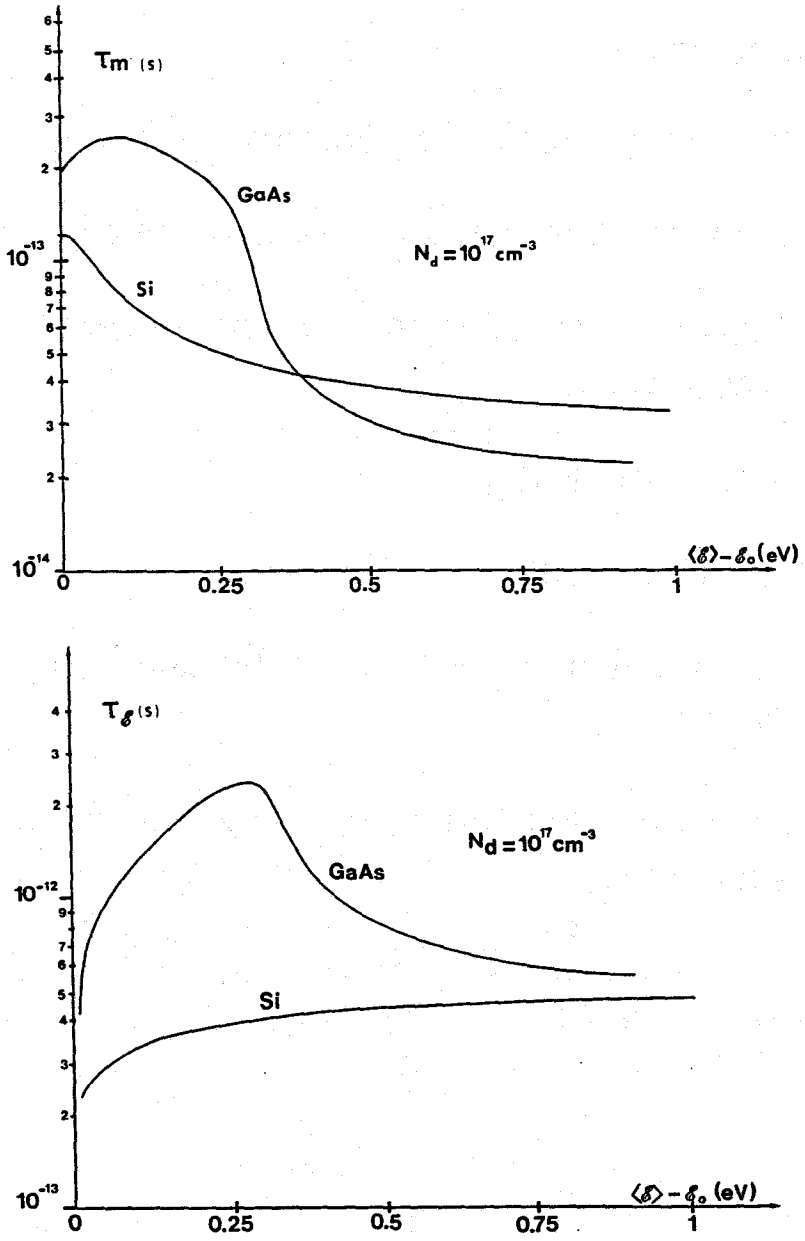

from E. Constant, Hot Electron Transport in Semiconductors, Springer-Verlag, 1985

Momentum and energy relaxation times for Si and GaAs

Carrier transport modelling
Drift-Diffusion formulation

Assume the carriers are always in equilibrium with the electric field

- mobility etc. may be written as functions of electric field

Carriers gain no energy from the field

- energy conservation equation may be eliminated

Using $J_n = nv_n$, $p_n = m^* v_n$ and $\mu_n = q\tau_m m^*$, we can write the momentum conservation equation as

$$\tau_m \frac{\partial J_n}{\partial t} + J_n = q\mu_n n \left[\frac{1}{n}\nabla\left(n\frac{k_B T}{q}\right) - \nabla\psi\right]$$

If we assume the momentum relaxation time is much less than the time scale of changes in the current, we have

$$J_n \gg \tau_m \frac{\partial J_n}{\partial t}$$

Employing the Einstein relations, for mobility and diffusivity yields the drift-diffusion expression for electron current

$$J_n = -q\mu_n n\nabla\psi + qD_n\nabla n$$

similarly for holes

$$J_p = -q\mu_p p\nabla\psi - qD_p\nabla p$$

Carrier transport modelling
Hydrodynamic formulation

Using the drifted Maxwellian distribution function, we may integrate the BTE over momentum space to generate "conservation" equations

i.e. for electrons:

- conservation of particles

$$\frac{\partial n}{\partial t} = \nabla \cdot (n v_n) = n_{scat}$$

- conservation of momentum

$$\frac{\partial p_n}{\partial t} = \nabla \cdot (v_n p_n) - qn\nabla\psi + \nabla(nk_B T_n) = p_{nscat}$$

- conservation of energy

$$\frac{\partial w_n}{\partial t} + \nabla \cdot (v_n w_n) - qnv_n\nabla\psi + \nabla \cdot (v_n nk_B T_n) - \nabla \cdot (\kappa_n \nabla T_n) = w_{nscat}$$

Similar equations may be derived for holes

Due to the symmetry of the drifted Maxwellian, heat conduction terms ($\kappa_n \nabla T_n$) must be added on an ad hoc basis

Carrier transport modelling
The one carrier model

For a CCD in normal operation, current flow is due to electrons only

- given and analytic expression for the hole concentration, we can eliminate the hole continuity equation
- this reduces the number of equations by a third

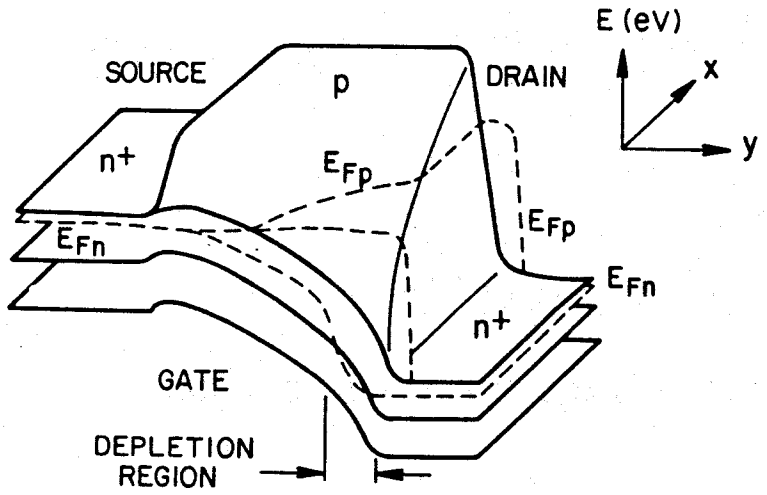

from Pao and Sah, Solid-State Electonics v9, 1966

If the hole current is zero, the quasi-Fermi level is flat

Carrier transport modelling
Drift-Diffusion formulation

We retain the continuity equations and Poisson:

$$\frac{\partial n}{\partial t} = \frac{1}{q}\nabla \cdot J_n - R$$

$$-\frac{\partial p}{\partial t} = \frac{1}{q}\nabla \cdot J_p - R$$

$$\nabla^2 \psi + \frac{q}{\epsilon}(p - n + N_D - N_A) = 0$$

$$J_n = -q\mu_n n \nabla \psi + qD_n \nabla n$$

$$J_p = -q\mu_p p \nabla \psi - qD_p \nabla p$$

Carrier transport modelling
The zero carrier model

For very low currents, we may eliminate both continuity equations

- requires insignificant non-equilibrium carrier density

Using the electron quasi-Fermi level ϕ_p

$$n = n_i e^{(\psi-\phi_n)/\phi_T}$$

Poisson's equation becomes

$$\nabla^2\psi + \frac{q}{\epsilon}\left[n_i e^{(\phi_p-\psi)/\phi_T} - n_i e^{(\psi-\phi_n)/\phi_T} + N_D - N_A\right] = 0$$

Analytic formulas may be used to determine small current flow

- i.e. subthreshold conduction

$$I_D = \frac{q\mu V_t^2 N_D}{E} \frac{1}{\int_0^L \exp\{\psi_0 - \psi(x,y)\}dx}$$

Carrier transport modelling
The one carrier model

We can write the hole concentration as

$$p = n_i e^{(\phi_p - \psi)/\phi_T}$$

The hole quasi-Fermi level ϕ_p is set by the boundary conditions

The drift-diffusion model now becomes

$$\nabla^2 \psi + \frac{q}{\epsilon}\left[n_i e^{(\phi_p - \psi)/\phi_T} - n + N_D - N_A\right] = 0$$

$$\frac{\partial n}{\partial t} = \frac{1}{q}\nabla \cdot J_n$$

$$J_n = -q\mu_n n \nabla \psi + qD_n \nabla n$$

- note Poisson's equation is now nonlinear

Carrier transport modelling
Summary

Drift-diffusion formulation

- carriers are in equilibrium with the electric field
- carriers do not gain energy
- time scales of interest must be $>$ relaxation times
- invalid for deep sub-micron work, high electric fields and short time scales

Carrier transport modelling
Summary

Boltzmann transport equation

- requires effective mass approximation
- carriers treated as classical particles
- collisions are instantaneous
- invalid for dimensions $<$ a few hundred Ang., frequencies above 10^{12} Hz, fields $>$ 10 MV/cm
- required for studies of extremely energetic carriers

Hydrodynamic formulation

- assumes a drifted Maxwellian distribution function and a simple band structure
- scattering in energy and momentum approximated by relaxation times
- requires high carrier concentrations
- will model non-stationary phenomena such as velocity overshoot

Modeling Physical Properties
Mobility

Lattice vibrations

- strong temperature dependence, mobility increases with decreasing temperature
- power law expressions are popular

$$\mu^L = \mu_0 \left[\frac{T}{300}\right]^{-\alpha}$$

or

$$\frac{1}{\mu^L} = \frac{1}{A\left[\frac{T}{300}\right]^{-\beta}} + \frac{1}{B\left[\frac{T}{300}\right]^{-\gamma}}$$

A wide variety of variations are available

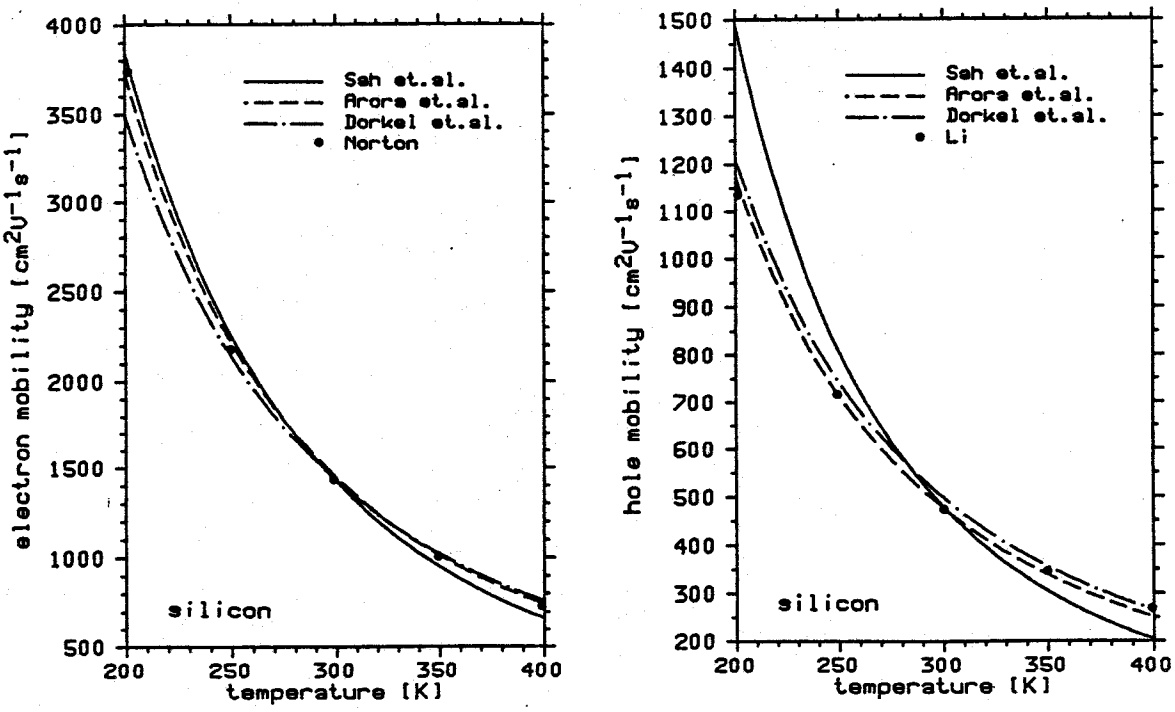

from Selberherr, Analysis and Simulation of Semiconductor Devices, Springer-Verlag, 1984

Modeling Physical Properties
Mobility

Anything which interupts the perfect periodic nature of the crystal lattice will reduce the mobility

Major effects for CCDs:

- lattice vibrations (acoustic phonons)
- ionized impurity scattering
- surface scattering (for surface channel CCDs)
- velocity saturation (optical phonons, high fields)

Detailed models based on perturbation theory and Fermi's golden rule are available but are too complex for general use

Simple analytic expressions are more popular

Modeling Physical Properties
Mobility

Surface scattering

- due to oxide charges, dipole scattering from hydrogen bonds and surface roughness

Yamaguchi

$$\mu^S = \mu^{LI} [1 + \alpha E_t]^{-1/2}$$

Selberherr

$$\mu^S = \mu^{LI} \left[\frac{x + x_0}{x + bx_0} \right]$$

Nishida and Sah

$$\mu^S = \frac{A}{E_t^\beta}$$

Modeling Physical Properties
Mobility

Ionized impurities

- introduces a random Coulombic potential
- mobility increases with increasing temperature

Caughey and Thomas

$$\mu^{LI} = \mu_0 + \frac{\mu^L - \mu_0}{1 + \left[\frac{N}{N_0}\right]^{\alpha}}$$

Scharfetter and Gummel

$$\mu^I = A\left[1 + \frac{N_0}{N}\right]$$

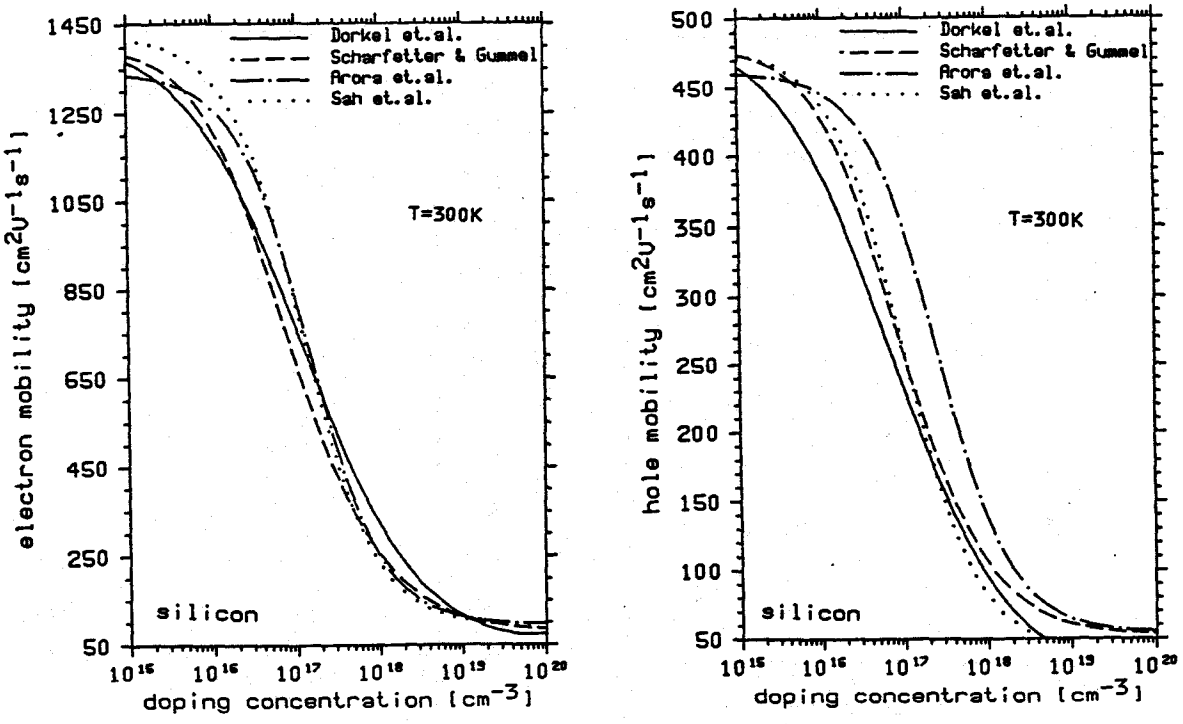

from Selberherr, Analysis and Simulation of Semiconductor Devices, Springer-Verlag, 1984

Modeling Physical Properties
Mobility

Velocity saturation

- all these saturation models assume equilibrium with the electric field
- in the hydrodynamic model, we can simulate non-equilibrium effects by making the mobility a function of the carrier energy
- usually done by creating an effective field parameter i.e. a relationship between the carrier energy and electric field

Modified Caughey-Thomas

$$\mathcal{E}(W_n) = \frac{W_n - W_l}{2v_{sat}q\tau_{wn}} + \left\{\left[\frac{W_n - W_l}{2v_{sat}q\tau_{wn}}\right]^2 + \frac{W_n - W_l}{q\mu_0\tau_{wn}}\right\}^{\frac{1}{2}}$$

Conwell temperature model

$$\mathcal{E}(W_n) = \frac{v_{sat}}{\mu_0}\left[\frac{W_n - W_l}{W_l}\right]^{\frac{1}{2}}$$

Modeling Physical Properties
Mobility

Velocity saturation

- Energy gained by the carriers from the electric field is quickly transfered to the lattice (optical phonons)

Most expressions are based on a ratio of the electric field to a critical field

$$\mu_{sat} = \frac{\mu^{LI}}{\left[1 + \left(\frac{E}{E_c}\right)^{\beta}\right]^{\frac{1}{\beta}}}$$

- strictly speaking, the quasi-Fermi level should be used in place of the field

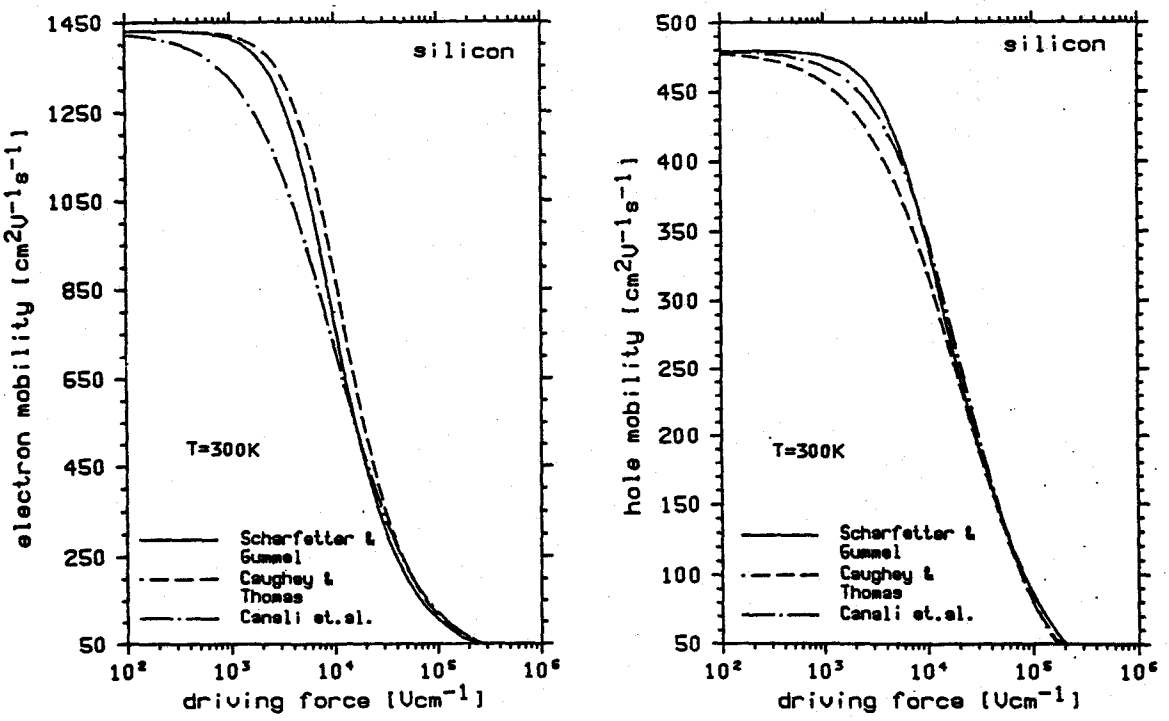

from Selberherr, Analysis and Simulation of Semiconductor Devices, Springer-Verlag, 1984

Modeling Physical Properties
Generation-Recombination

Optical generation

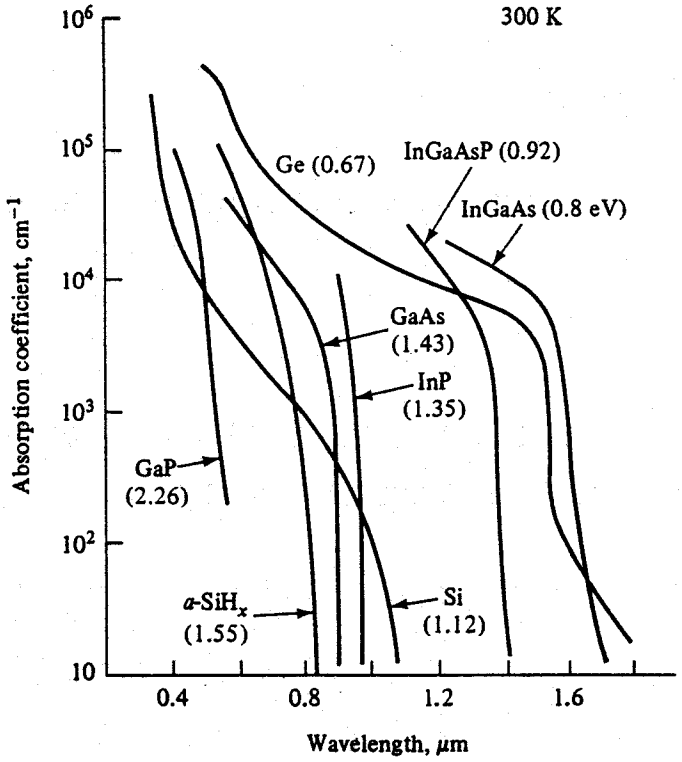

from Yang, Microelectronic Devices, McGraw-Hill, 1988

G_{opt} is based on the incident photon flux ϕ_0 and the absorption coefficient α

$$G_{opt} = \phi_0 \alpha e^{-\alpha x}$$

Modeling Physical Properties
Generation-Recombination

We require optical generation, bulk and surface recombination for low-frequency limits and impact ionization for junction breakdown

Bulk recombination

$$R_{srh} = \frac{np - n_i^2}{\tau_p (n + n_i) + \tau_n (p + n_i)}$$

- lifetimes are function of impurity concentrations

$$\tau_n = \frac{\tau_{n0}}{1 + \frac{N}{N_0}} \qquad \tau_p = \frac{\tau_{p0}}{1 + \frac{N}{N_0}}$$

Surface recombination

- uses the same form as bulk recombination only written in terms of recombination velocities instead of carrier lifetimes

$$R_{sur} = \frac{np - n_i^2}{(1/s_p)(n + n_i) + (1/s_n)(p + n_i)}$$

Process Simulation

We require accurate impurity profiles as well as detailed structural information

Ion implantation

$$N(x,y) = \frac{Q_0}{\sqrt{2\pi}\delta R_p} \exp\left\{\left[-\frac{1}{2}\left(\frac{x-R_p}{\delta R_p}\right)^2\right]\left[\frac{1}{\sqrt{\pi}}\text{erfc}\left(\frac{y-a}{\sqrt{2}\delta R_t}\right)\right]\right\}$$

Diffusion

- constant source

$$N(x,t) = N_0 \text{erfc}\left[\frac{x}{2\sqrt{Dt}}\right]$$

- limited source

$$N(x,t) = \frac{Q_0}{\sqrt{\pi Dt}} \exp\left\{-\left(\frac{x}{2\sqrt{Dt}}\right)^2\right\}$$

Modeling Physical Properties
Generation-Recombination

Impact ionization

- usually modelled as proportional to the particle current

$$G_{ii} = \alpha_n \frac{J_n}{q} + \alpha_p \frac{J_p}{q}$$

- ionization coefficients are an exponential function of the electric field

$$\alpha = \alpha_0 e^{-B/E}$$

- in hydrodynamic simulation, it is better to express the coefficients in terms of the carrier energy

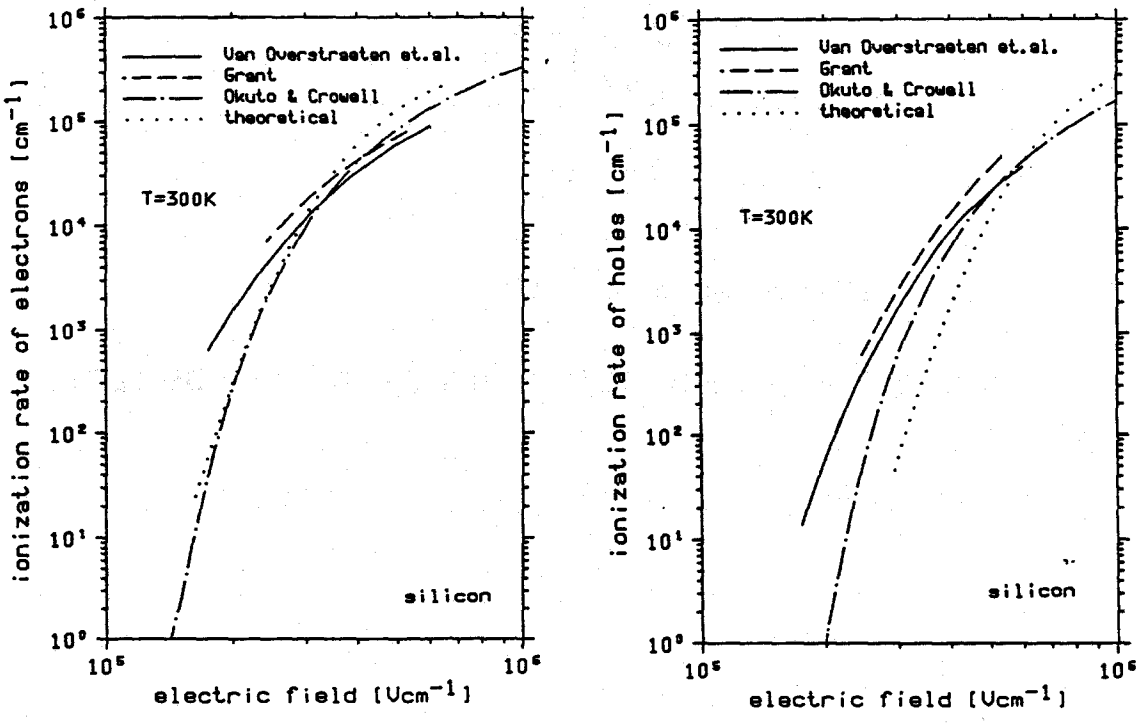

from Selberherr, Analysis and Simulation of Semiconductor Devices, Springer-Verlag, 1984

Equation Discretization

Discretization is based on the box integration method

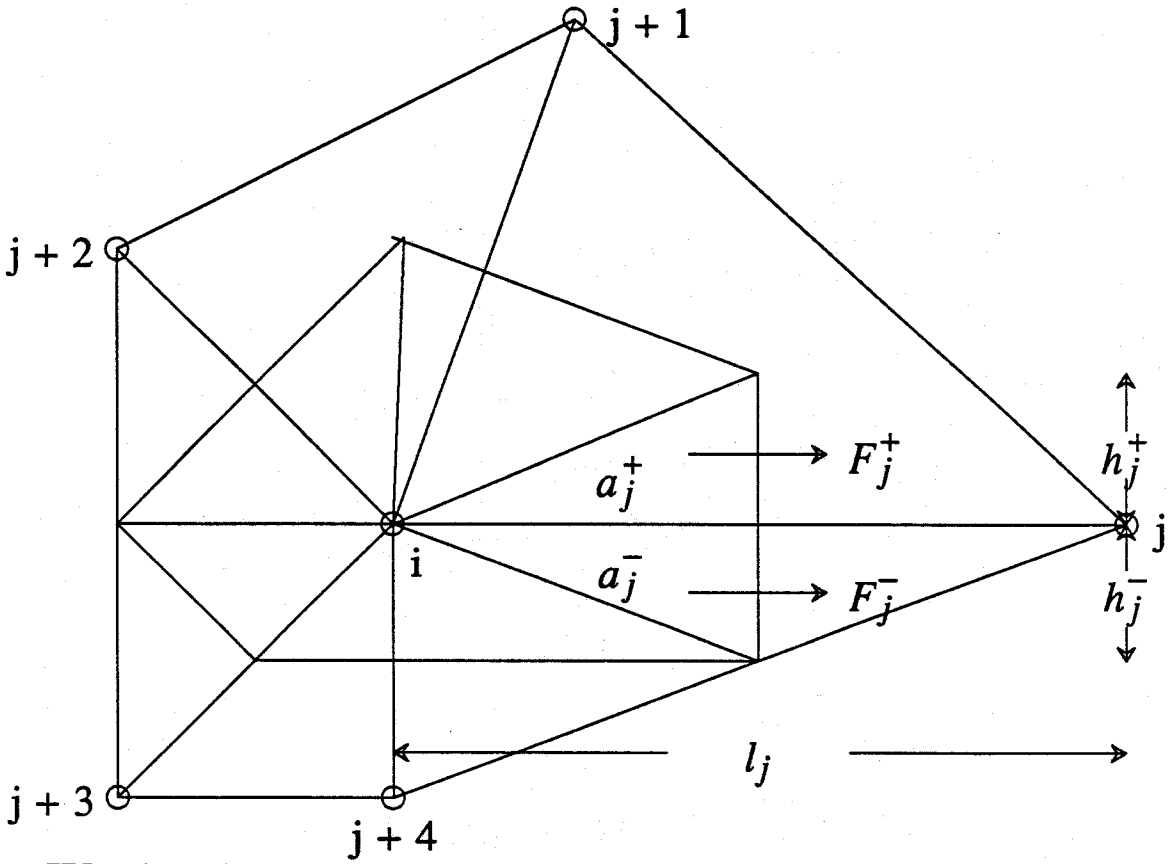

We develop a control volume for each grid node by intersecting the perpendicular bisectors of the grid lines.

Given a two-dimensional partial differential equation in point form:

$$\nabla \cdot \mathbf{F} = G$$

We integrate over this area and apply the divergence theorem to yield

$$\mathbf{F} \cdot d\mathbf{s} = \iint \mathbf{G} dA$$

Equation Discretization

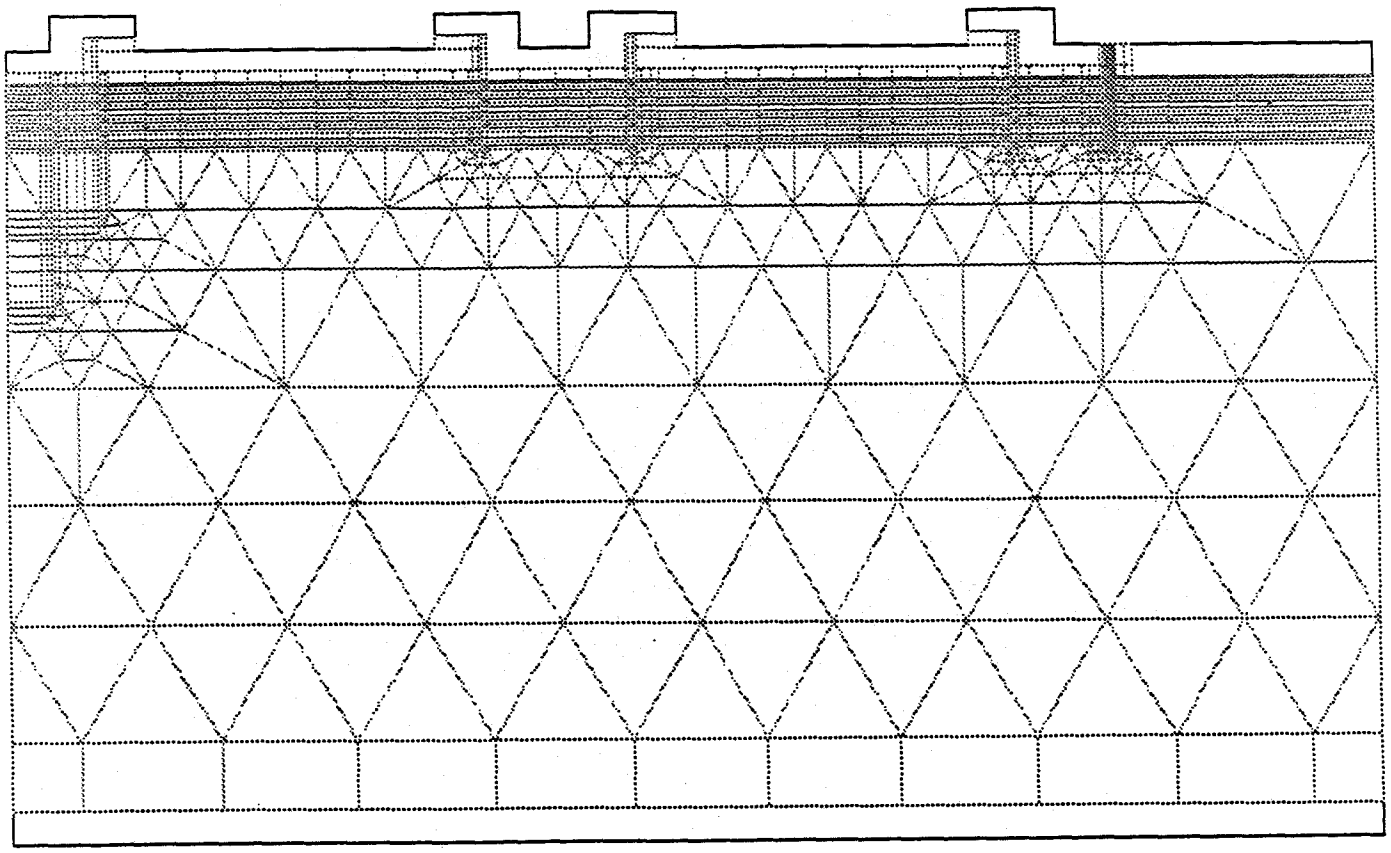

We convert differential equations to algebraic equations by discretizing over a grid

Equation Discretization

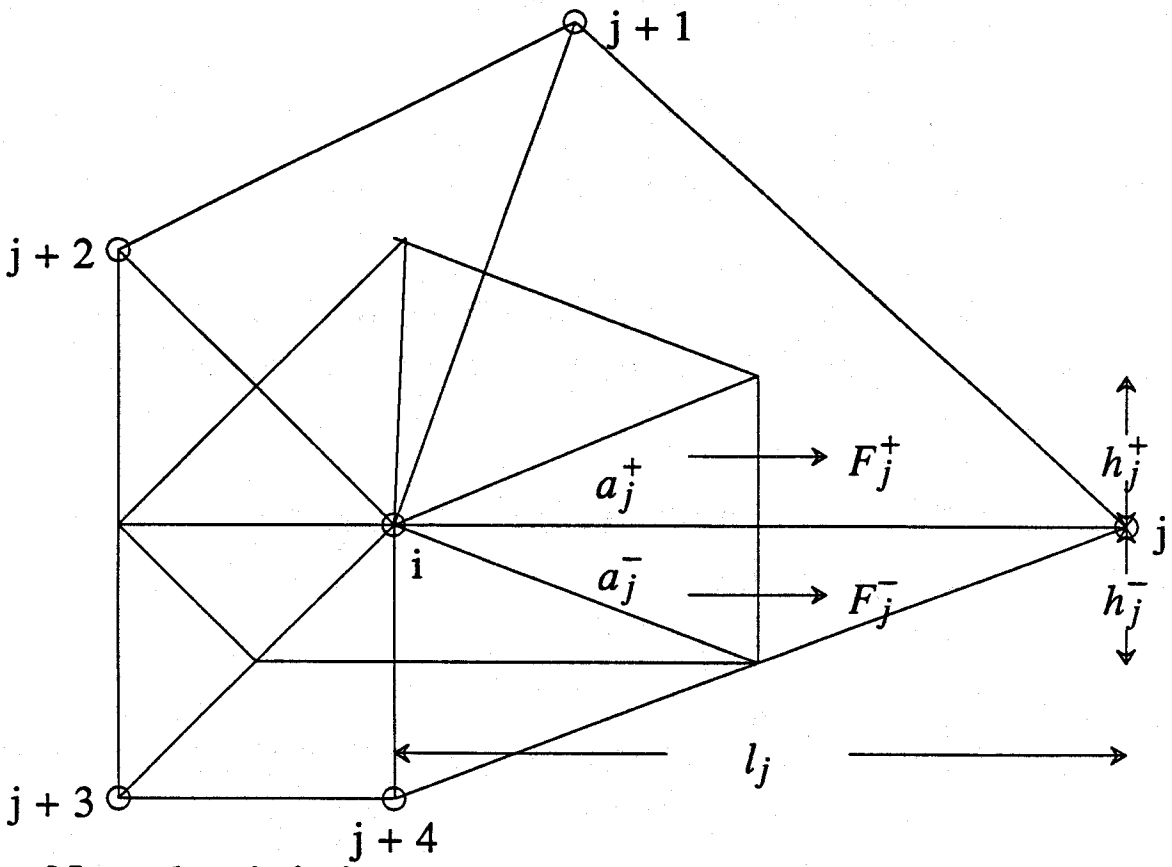

Note that it is important that the grid contain no obtuse angles, as this will lead to overlapping areas

Equation Discretization

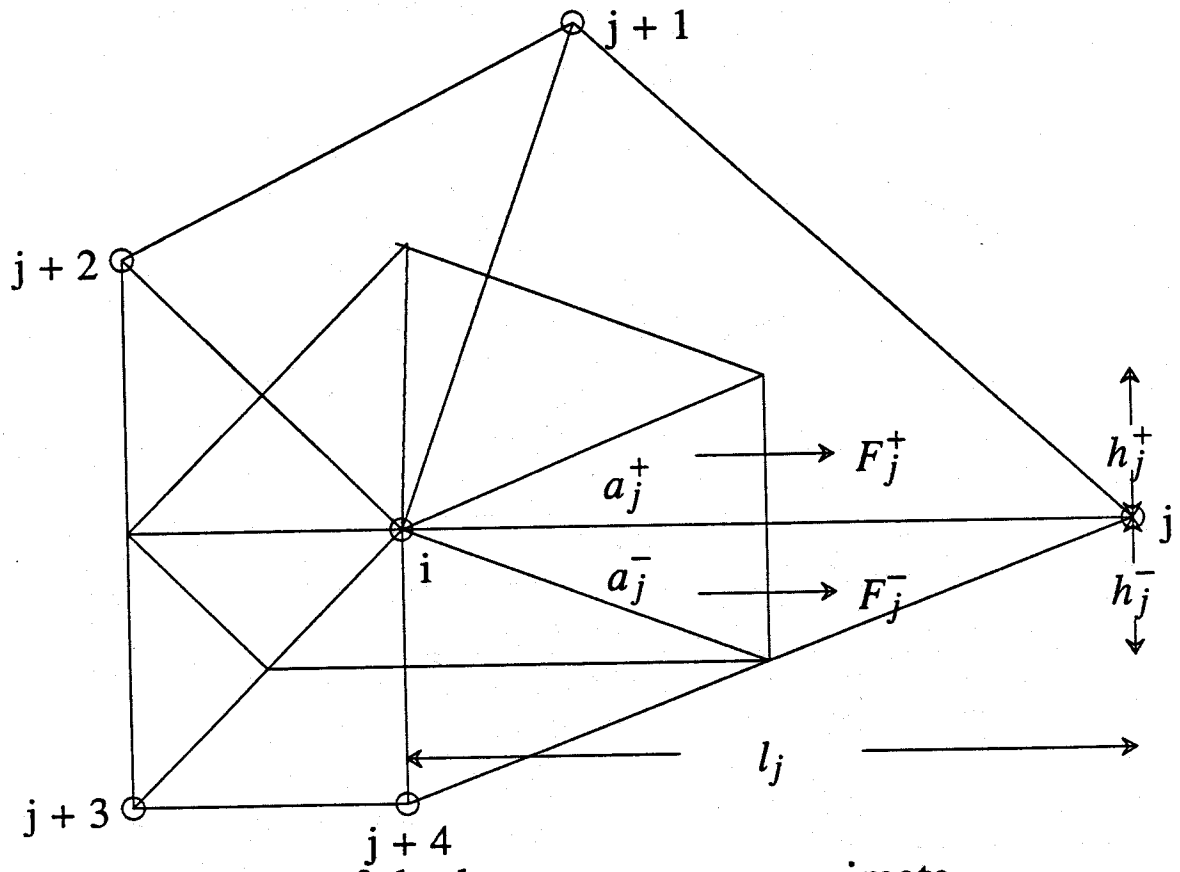

For one face of the box, we can approximate

$$F^+{}_j h^+{}_j + F^-{}_j h^-{}_j = G^+{}_j a^+{}_j + G^-{}_j a^-{}_j$$

Summing over all m faces, we have

$$\sum_{j=1}^{m} F^+{}_j h^+{}_j + F^-{}_j h^-{}_j = \sum_{j=1}^{m} G^+{}_j a^+{}_j + G^-{}_j a^-{}_j$$

Equation Discretization
The Drift-Diffusion Model

$$\frac{\partial n}{\partial t} - \frac{1}{q}\nabla\cdot\mathbf{J}_n + R = 0$$

We integrate using a simple backward Euler form:

$$\frac{\partial f}{\partial t} = \frac{f_{k+1} - f_k}{\Delta t} .$$

yielding

$$\frac{1}{q}\sum_{j=1}^{n}\left[h_j^+ + h_j^-\right]J_{njk+1} - \left[R_{ik+1} + \frac{n_{ik+1} - n_{ik}}{\Delta t}\right]\sum_{j=1}^{n}\left[a_j^+ + a_j^-\right] = 0 .$$

This equation is implemented using $1/\Delta t$ as a variable. By setting $1/\Delta t = 0$, we have the steady-state model.

Equation Discretization
The Drift-Diffusion Model

$$\nabla^2\psi - \frac{q}{\varepsilon}\left[N + p - n\right] = 0$$

To apply box integration to bulk semiconductor, assume the material across the box is homogeneous i.e. $F_j^+ = F_j^-$ and $G_j^+ = G_j^-$.

Using $\mathbf{D} = \varepsilon\mathbf{E}$ and a simple difference form for the field in terms of the potential,

$$\sum_{j=1}^{n}\left[\frac{h_j^+ + h_j^-}{l_j}\right]\left[\psi_j - \psi_i\right] + \frac{q}{\varepsilon}\left[p_i - n_i + N_i\right]\sum_{j=1}^{n}\left[a_j^+ + a_j^-\right] = 0\,.$$

Solution Methods

Newton Iteration

Given a set of equations $\mathbf{F} = F_1, F_2, \ldots F_n$

in the variables $\mathbf{x} = x_1, x_2, \ldots x_n$

- at each iteration k we solve the linear system

$\mathbf{J}_k \, \Delta\mathbf{x}_k = \mathbf{F}(\mathbf{x}_k)$, where $\mathbf{J}(\mathbf{x}_k)$ is the Jacobian matrix

$$J = \begin{bmatrix} \frac{\partial F_1}{\partial x_1} & \frac{\partial F_1}{\partial x_2} & \cdots & \frac{\partial F_1}{\partial x_n} \\ \frac{\partial F_2}{\partial x_1} & \frac{\partial F_2}{\partial x_2} & \cdots & \frac{\partial F_2}{\partial x_n} \\ \vdots & \vdots & & \vdots \\ \frac{\partial F_n}{\partial x_1} & \frac{\partial F_n}{\partial x_2} & \cdots & \frac{\partial F_n}{\partial x_n} \end{bmatrix}$$

evaluated at $\mathbf{x}_k$.

- The solution estimate $\mathbf{x}_k$ is updated by

$\mathbf{x}_{k+1} = \mathbf{x}_k + \Delta\mathbf{x}_k$.

- This process continues until both $||\mathbf{F}(\mathbf{x}_k)||_2$ and $||\Delta\mathbf{x}_k||_2$ are suitably small.

Equation Discretization

The Drift-Diffusion Model

The Scharfetter-Gummel approximation for the current is

$$J_{nik+1} = -q\frac{\mu_{njk+1}}{l_j}\Delta\psi_{jk+1}\left[\frac{n_{ik+1}}{1-e^{-\Delta\psi_{jk+1}/\phi_T}} + \frac{n_{jk+1}}{1-e^{\Delta\psi_{jk+1}/\phi_T}}\right]$$

where $\Delta\psi_{jk+1} = \psi_{jk+1} - \psi_{ik+1}$.

We implement this using the Bernoulli function

$$B(\Delta\psi_{jk+1}/\phi_T) = \frac{\Delta\psi_{jk+1}/\phi_T}{e^{\Delta\psi_{jk+1}/\phi_T} - 1}$$

yielding

$$J_{nik+1} = -q\frac{\phi_T\mu_{njk+1}}{l_j}\left[n_{ik+1}B(-\Delta\psi_{jk+1}/\phi_T) - n_{jk+1}B(\Delta\psi_{jk+1}/\phi_T)\right]$$

- For values of $x = \Delta\psi_{jk+1}/\phi_T$ close to zero, we approximate $B(x)$ as a truncated Taylor series.
- This formulation prevents numerical overflow due to a large $\Delta\psi$.

Solution Methods
Comparison

Gummel iteration

- requires only enough memory for each equation set
- simple formulation
- for very low currents, may eliminate continuity equations altogether
- linear convergence
- tends to diverge when coupling between equations is strong (high current)

Newton iteration

- requires enough memory for entire set of equations
- formulation is complex - generation of Jacobian elements
- functions well under a wide variety of device conditions
- quadratic convergence "sufficiently close" to the solution

Solution Methods

Gummel Iteration

We can write the drift-diffusion model in terms of the electron and hole quasi-Fermi levels:

$$F_1 = \nabla^2\psi + \frac{q}{\varepsilon}\left[N + n_i e^{-\beta(\psi-\phi_p)} - n_i e^{\beta(\psi-\phi_n)}\right],$$

$$F_2 = \nabla\cdot\left[\mu_n n_i e^{\beta(\psi-\phi_n)}\nabla\phi_n\right] - R = 0,$$

$$F_3 = \nabla\cdot\left[\mu_p n_i e^{-\beta(\psi-\phi_p)}\nabla\phi_p\right] + R = 0.$$

Given an initial estimate for the quasi-Fermi levels, solve F_1 for the potential ψ

Using ψ, solve F_2 and F_3 for new quasi-Fermi levels

Repeat until converged

The CHORD Simulator

All required device structure, grid and physical property information is stored in a simulation database

- each simulation task may be coded as an independent program
- data structures are bound to the tasks and not a large package

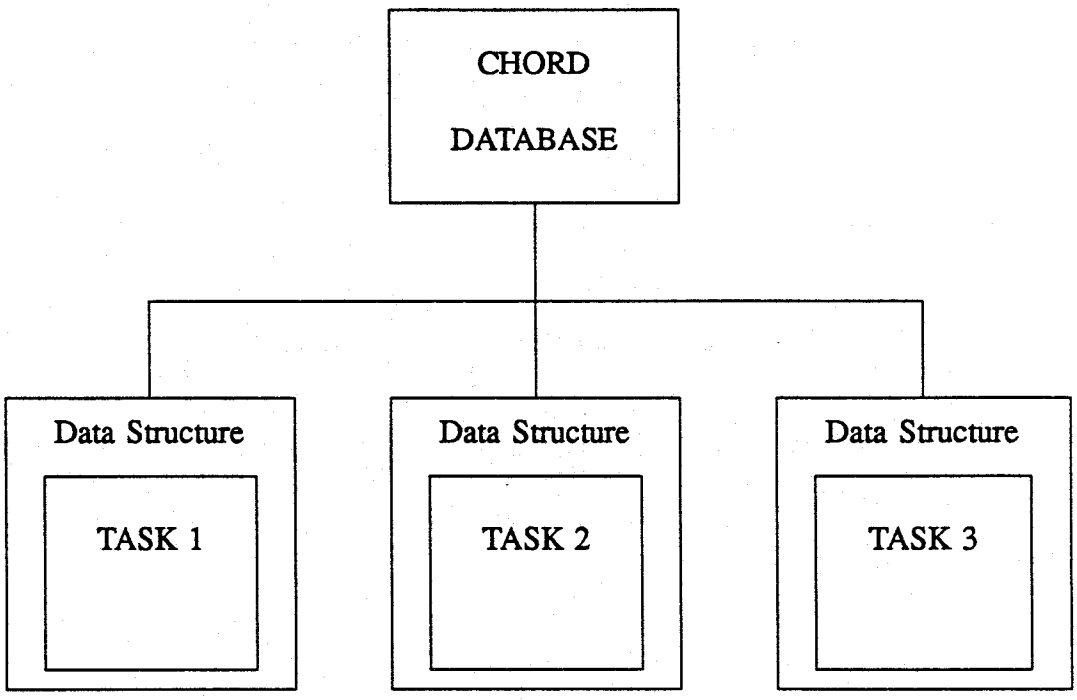

The CHORD Simulator

Most simulation tasks require access to a large amount of device information

- a grid mapped to the device boundaries
- what equations to set up and solve at each node or element
- physical properties of the materials
  - — doping
  - — interface charges
  - — fixed charge
  - — permitivities and permeabilities

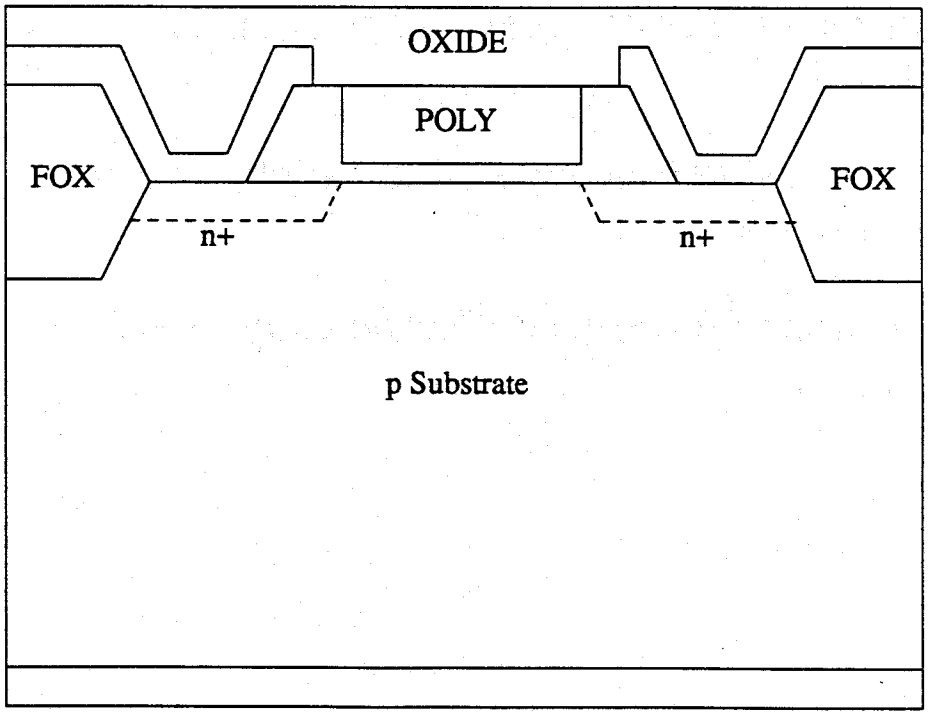

The CHORD Simulator

All device information is stored in a *configuration file*

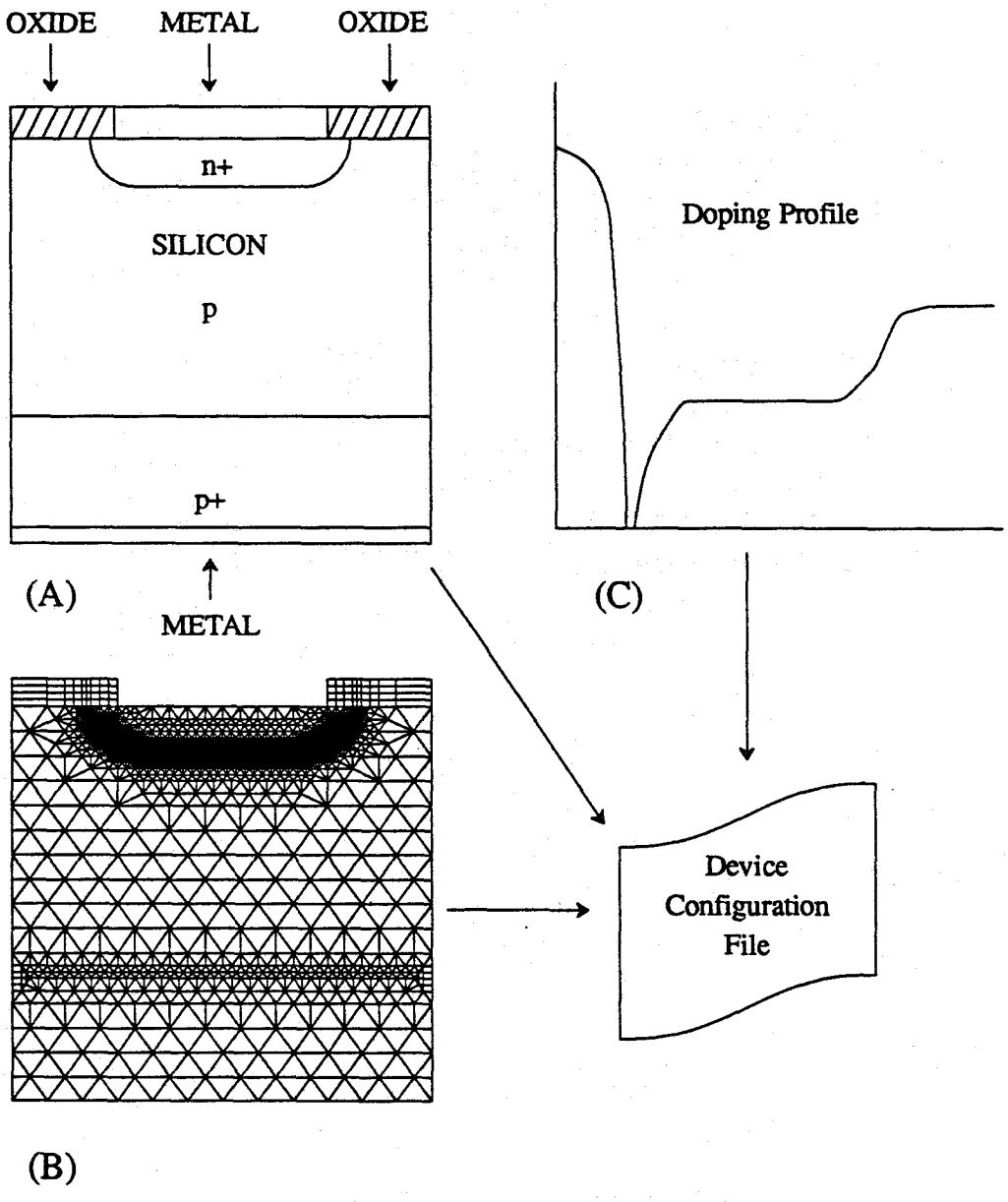

The CHORD Simulator

- the database is implemented as a *simulation server* using inter-process communication

- individual programs (clients) can connect to the server and obtain all required information without being integrated into a large simulation package

- server/client communication based on UNIX *sockets*

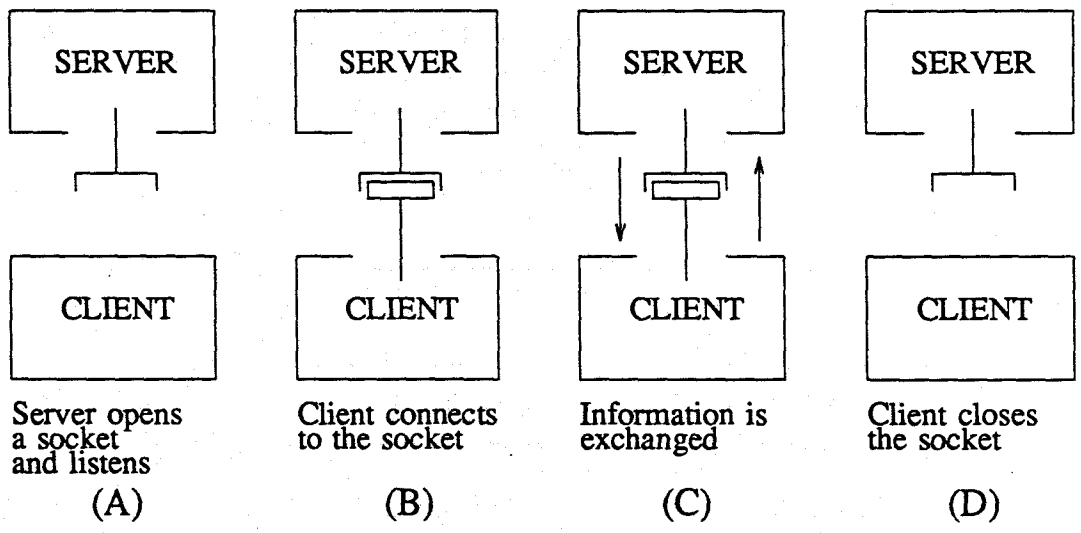

The CHORD Simulator

- connection may exist with the server and client on the same machine or on different machines

- the simulation database may run on a central machine with graphics-intensive operations performed on a small workstation and number-crunching on a larger CPU

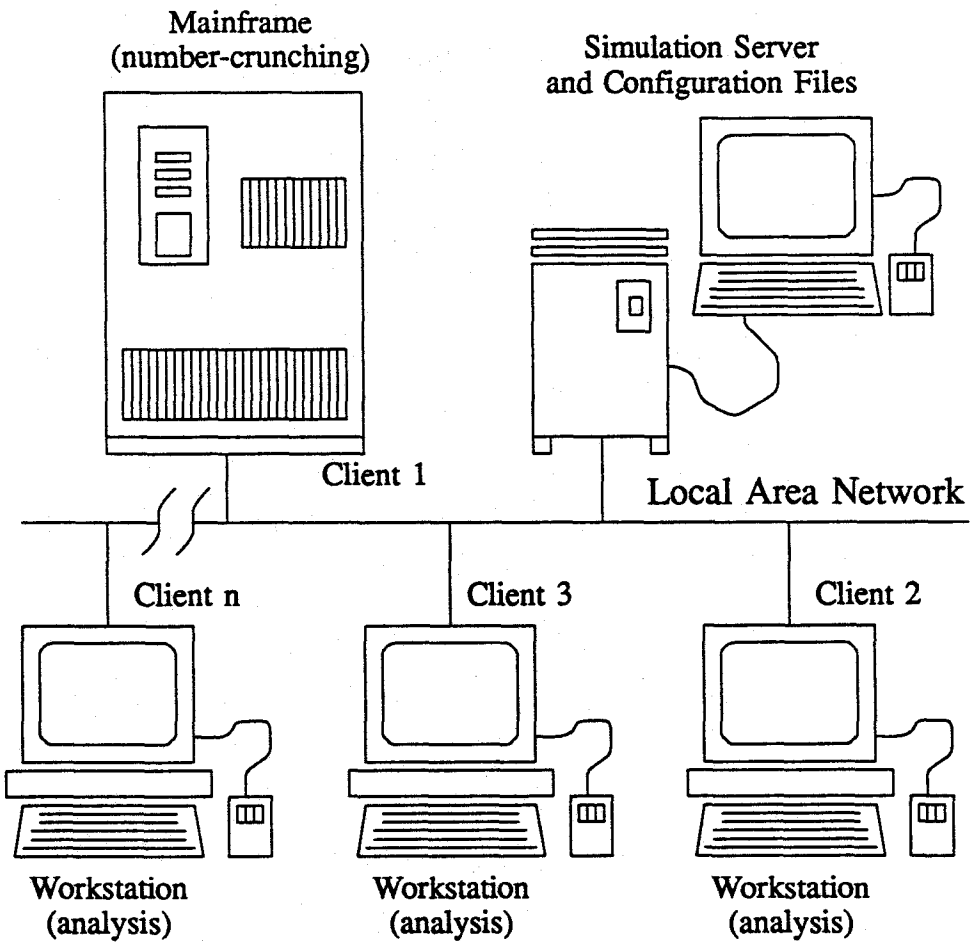

The CHORD Simulator

The configuration file is used to initialize the database

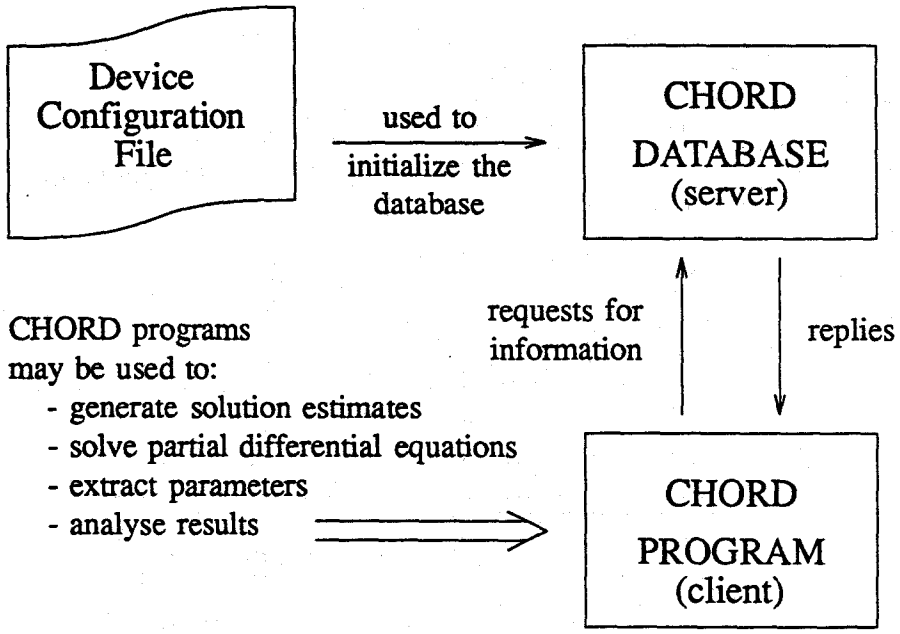

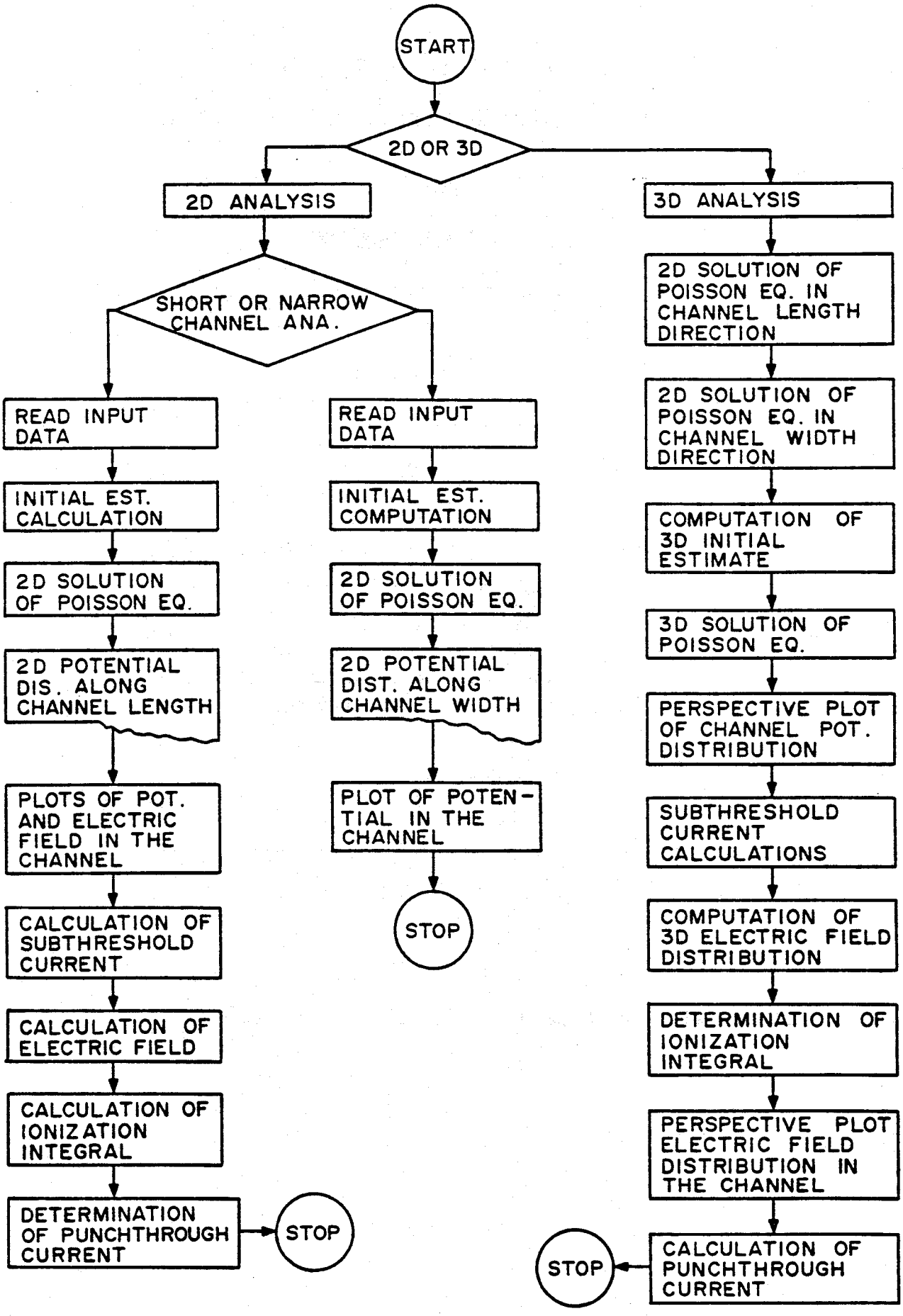
START
2D OR 3D
2D ANALYSIS
3D ANALYSIS
SHORT OR NARROW CHANNEL ANA.
READ INPUT DATA
INITIAL EST. CALCULATION
2D SOLUTION OF POISSON EQ.
2D POTENTIAL DIS. ALONG CHANNEL LENGTH
PLOTS OF POT. AND ELECTRIC FIELD IN THE CHANNEL
CALCULATION OF SUBTHRESHOLD CURRENT
CALCULATION OF ELECTRIC FIELD
CALCULATION OF IONIZATION INTEGRAL
DETERMINATION OF PUNCHTHROUGH CURRENT
STOP
READ INPUT DATA
INITIAL EST. COMPUTATION
2D SOLUTION OF POISSON EQ.
2D POTENTIAL DIST. ALONG CHANNEL WIDTH
PLOT OF POTEN-TIAL IN THE CHANNEL
STOP
2D SOLUTION OF POISSON EQ. IN CHANNEL LENGTH DIRECTION
2D SOLUTION OF POISSON EQ. IN CHANNEL WIDTH DIRECTION
COMPUTATION OF 3D INITIAL ESTIMATE
3D SOLUTION OF POISSON EQ.
PERSPECTIVE PLOT OF CHANNEL POT. DISTRIBUTION
SUBTHRESHOLD CURRENT CALCULATIONS
COMPUTATION OF 3D ELECTRIC FIELD DISTRIBUTION
DETERMINATION OF IONIZATION INTEGRAL
PERSPECTIVE PLOT ELECTRIC FIELD DISTRIBUTION IN THE CHANNEL
CALCULATION OF PUNCHTHROUGH CURRENT
STOP

WATMOS

WATMOS is a two or three-dimensional, zero-carrier simulator

- used to study potential distribution and subthreshold current flow in MOS devices
- based on finite difference orthogonal grids
- successive over-relaxation to solve Poisson's equation
- a variety of post-process data analysis is available

Simulation Results
One-Dimensional Drift-Diffusion

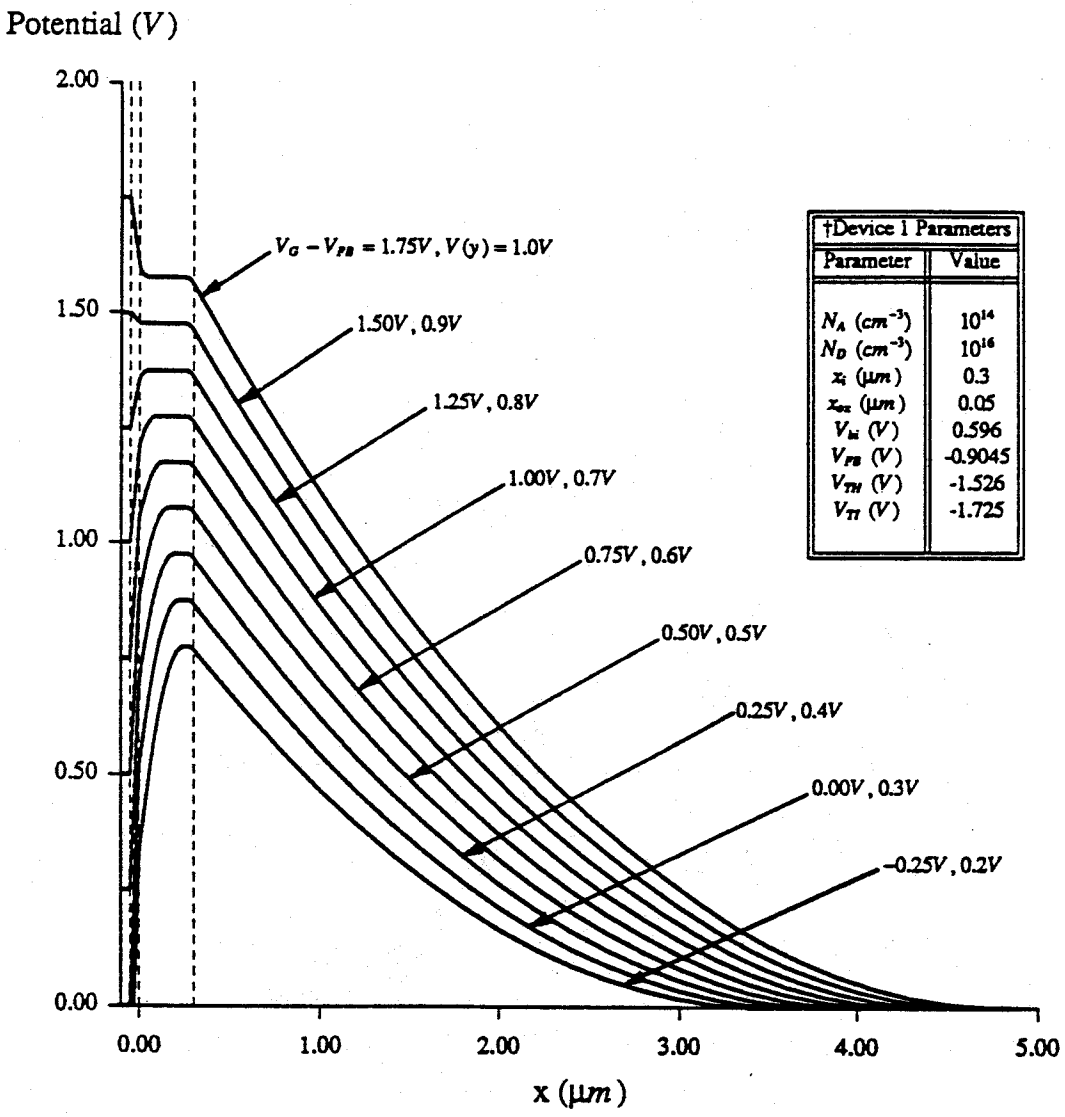

†Device 1 Parameters

Parameter	Value
N_A (cm^{-3})	10^{14}
N_D (cm^{-3})	10^{16}
x_j (μm)	0.3
x_{ox} (μm)	0.05
V_{bi} (V)	0.596
V_{FB} (V)	-0.9045
V_{TH} (V)	-1.526
V_{TT} (V)	-1.725

from Van der Tol and Chamberlain, IEEE Trans Elec Dev, ED-36, 1989

Simulation Results
One-Dimensional Drift-Diffusion

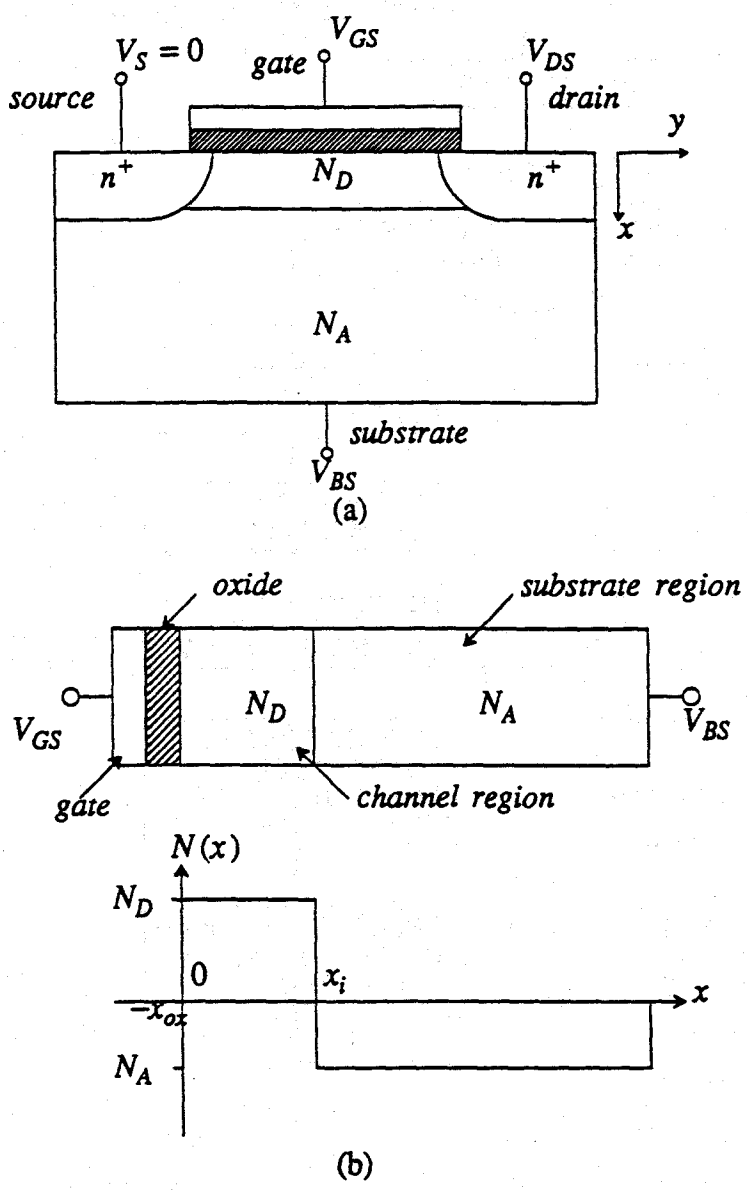

from Van der Tol and Chamberlain, IEEE Trans Elec Dev, ED-36, 1989

Simulation Results
Two-Dimensional Hydrodynamic

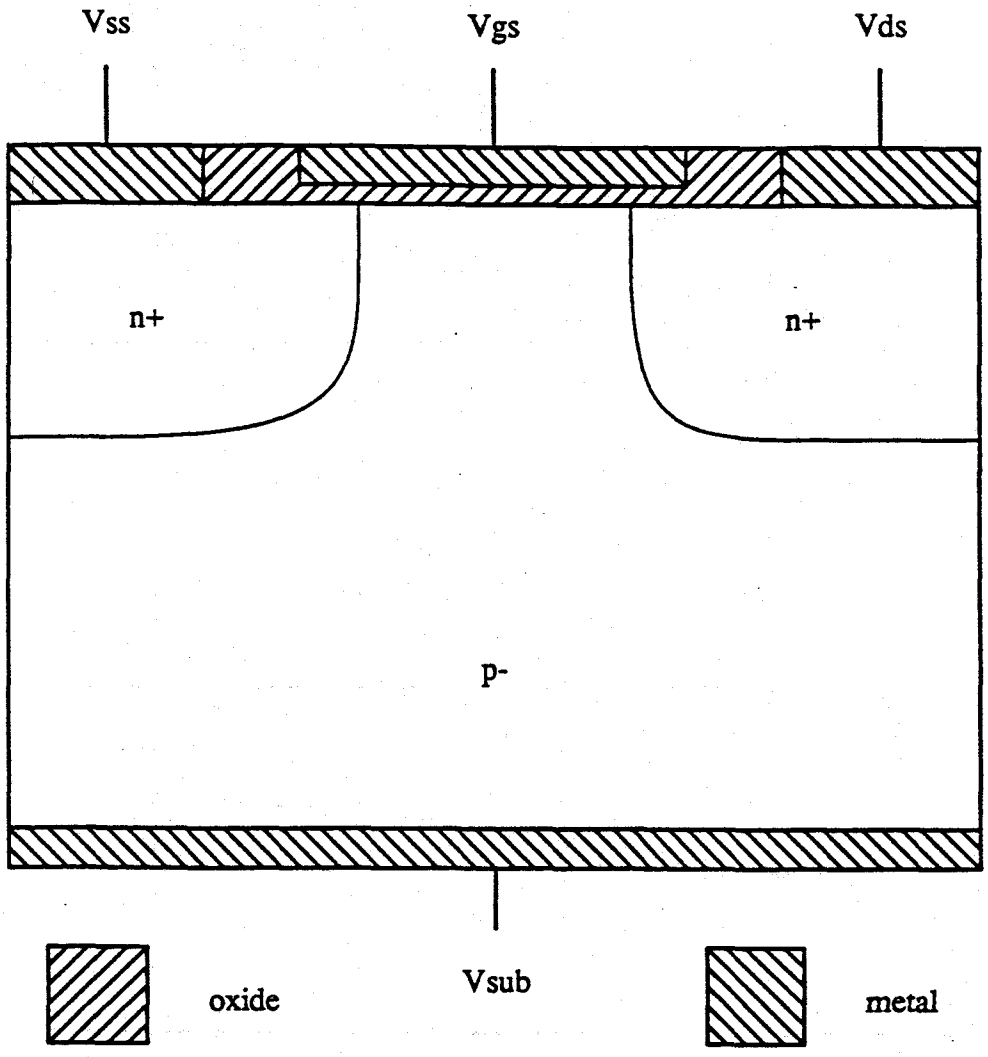

from Roberts, Modelling and Simulation of Small Geometry Silicon Devices, University of Waterloo

Layout of a 2 μm MOSFET

Simulation Results
One-Dimensional Drift-Diffusion

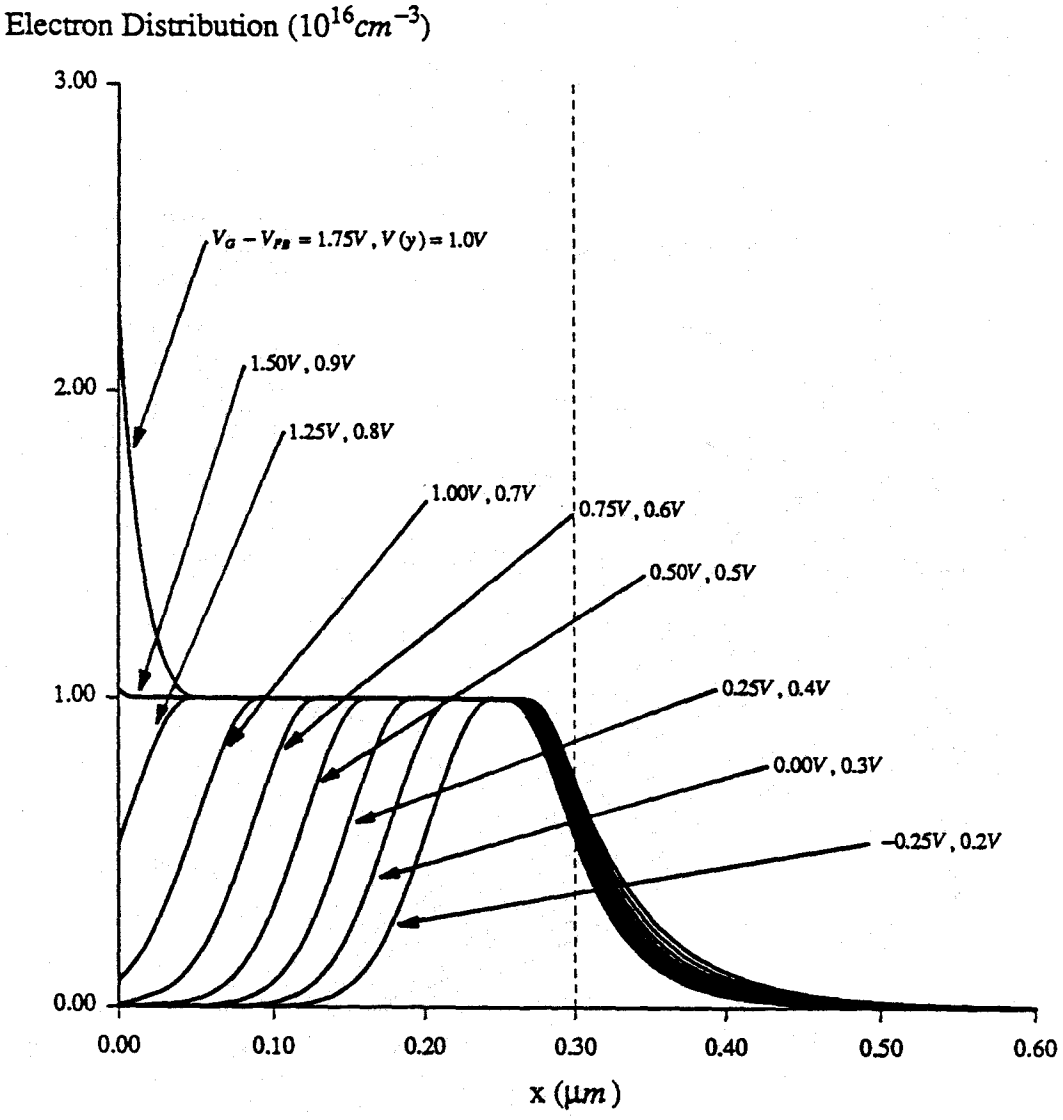

from Van der Tol and Chamberlain, IEEE Trans Elec Dev, ED-36, 1989

Simulation Results
Two-Dimensional Hydrodynamic

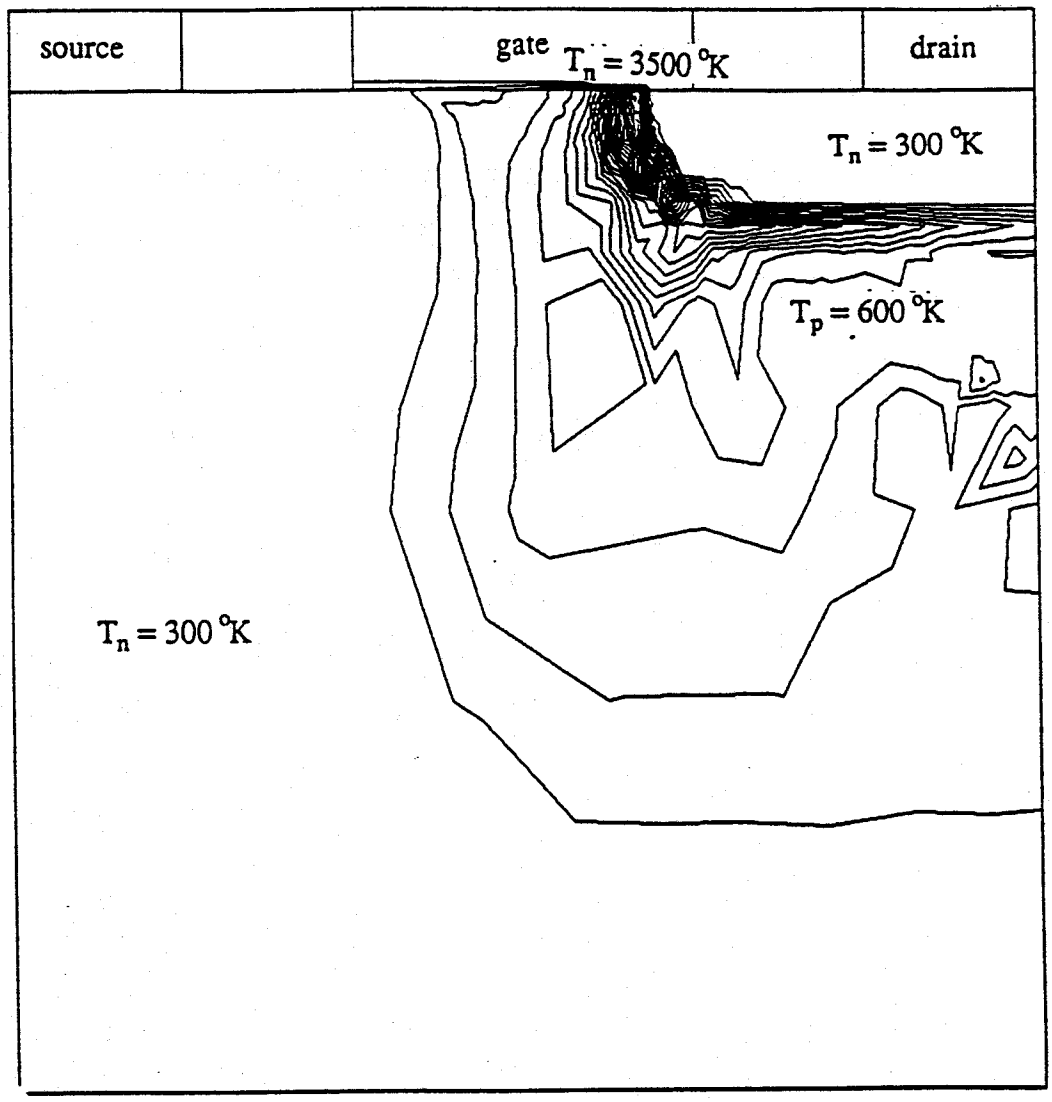

from Roberts, Modelling and Simulation of Small Geometry Silicon Devices, University of Waterloo

Electron temperature in saturation

Simulation Results
Two-Dimensional Hydrodynamic

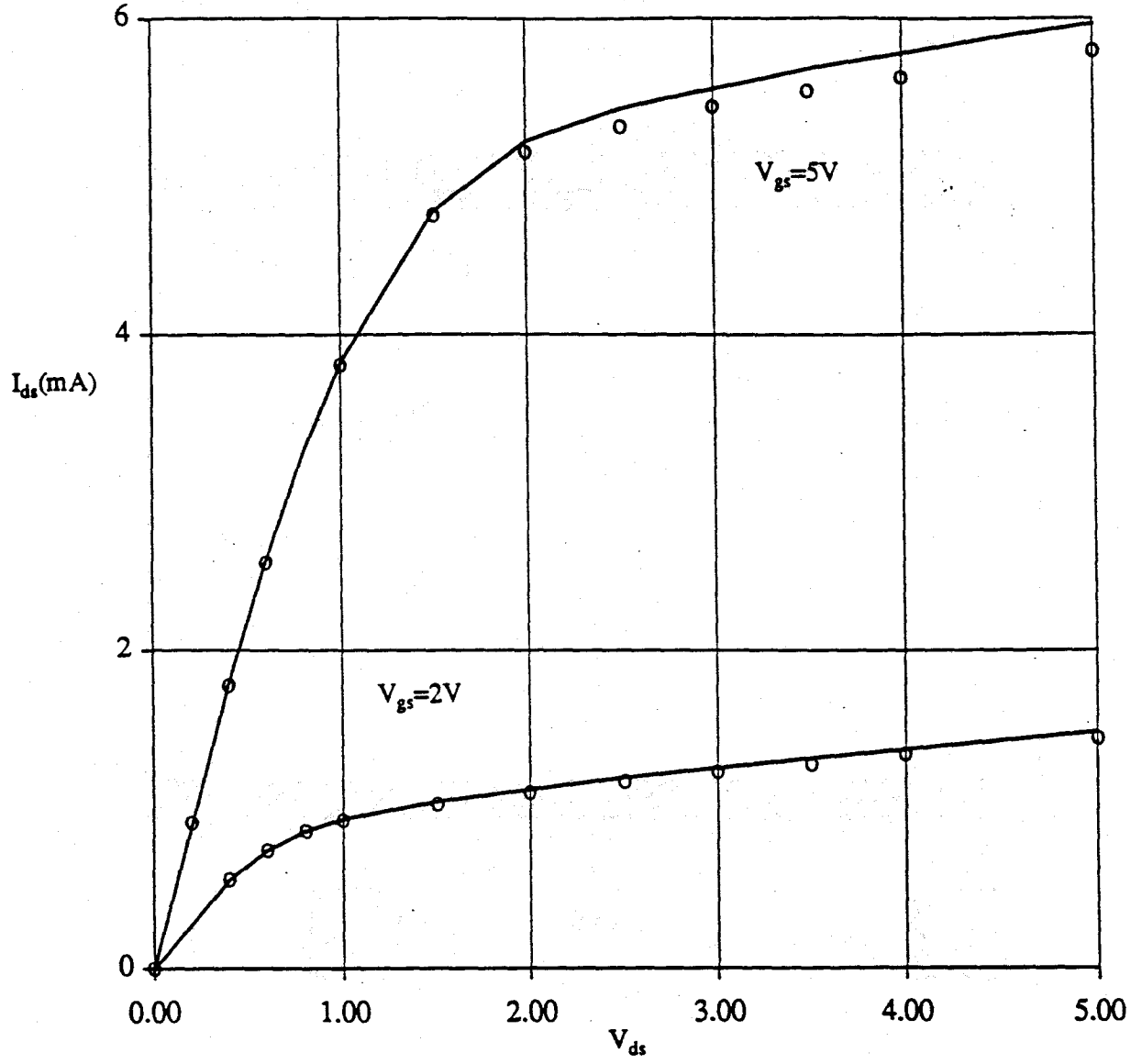

from Roberts, Modelling and Simulation of Small Geometry Silicon Devices, University of Waterloo

I-V characteristics, drift-diffusion (lines) and hydrodynamic (o)

- note the reduced channel length modulation

Simulation Results
Two-Dimensional Hydrodynamic

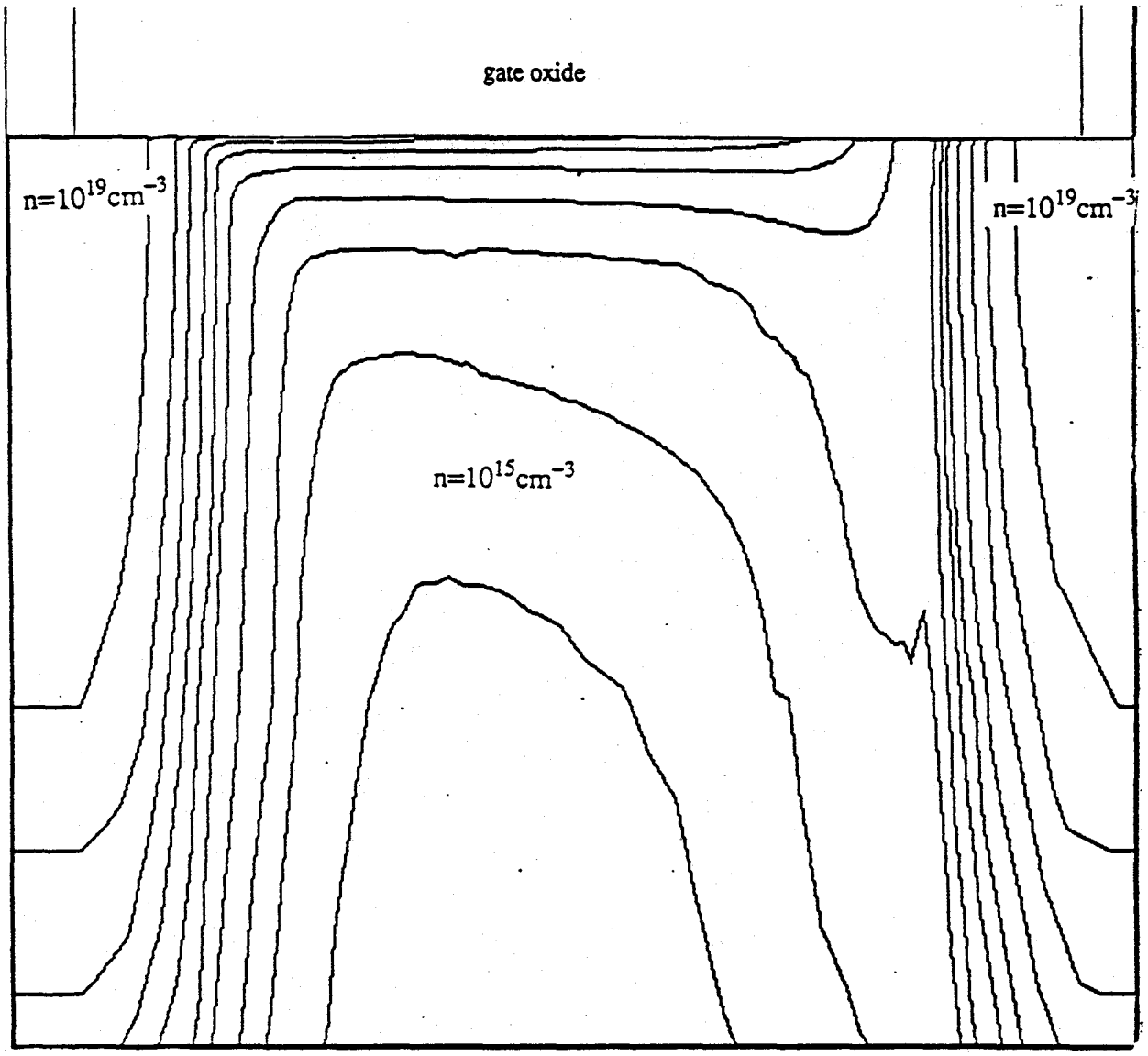

from Roberts, Modelling and Simulation of Small Geometry Silicon Devices, University of Waterloo

Electron concentration, hydrodynamic model

- note the carriers push farther into the bulk, increasing the effective channel length
- this reduces channel length modulation

Simulation Results
Two-Dimensional Hydrodynamic

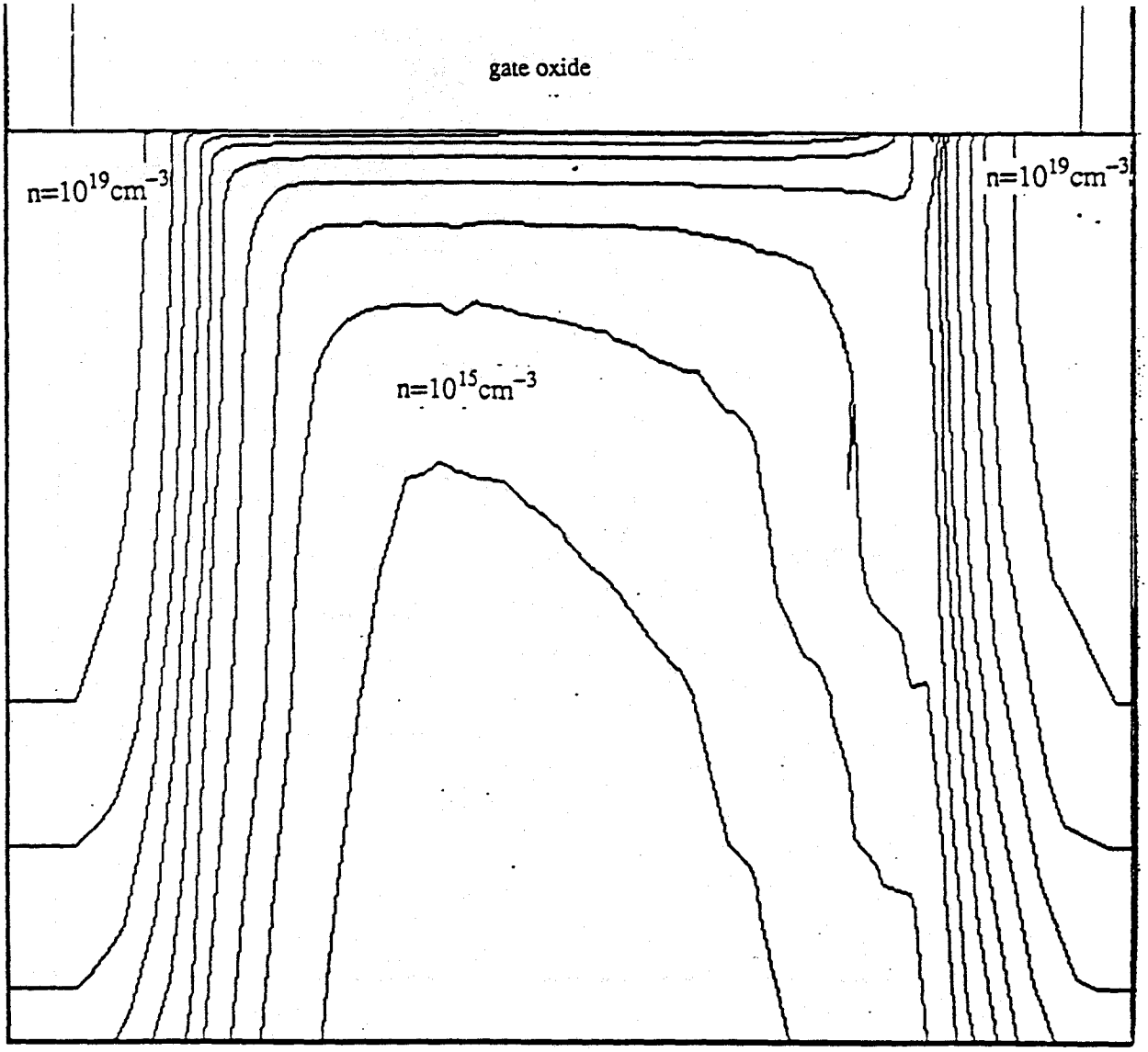

from Roberts, Modelling and Simulation of Small Geometry Silicon Devices, University of Waterloo

Electron concentration, drift-diffusion model

Simulation Results
Two-Dimensional Hydrodynamic

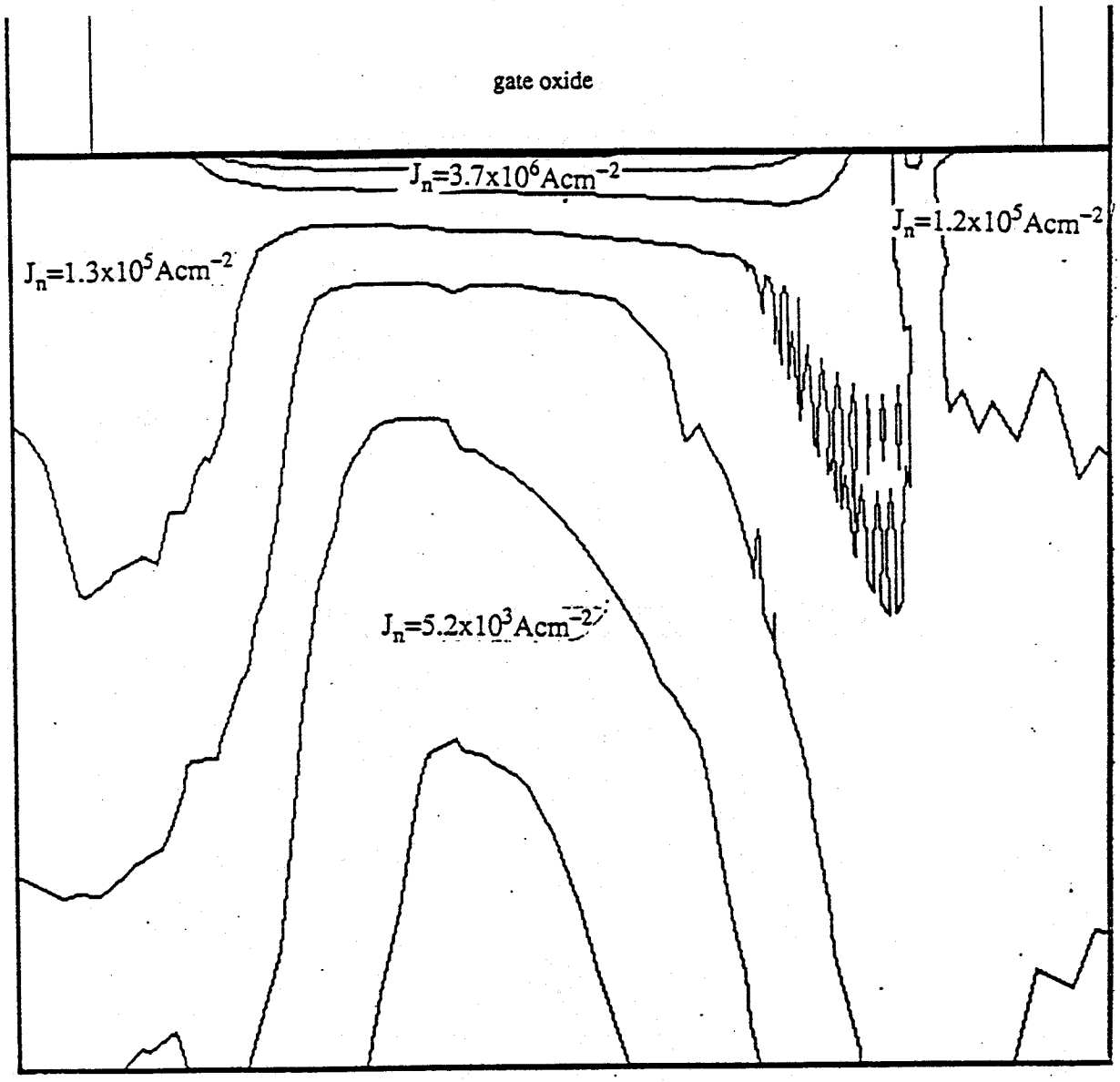

from Roberts, Modelling and Simulation of Small Geometry Silicon Devices, University of Waterloo

Current density, hydrodynamic model

Simulation Results
Two-Dimensional Hydrodynamic

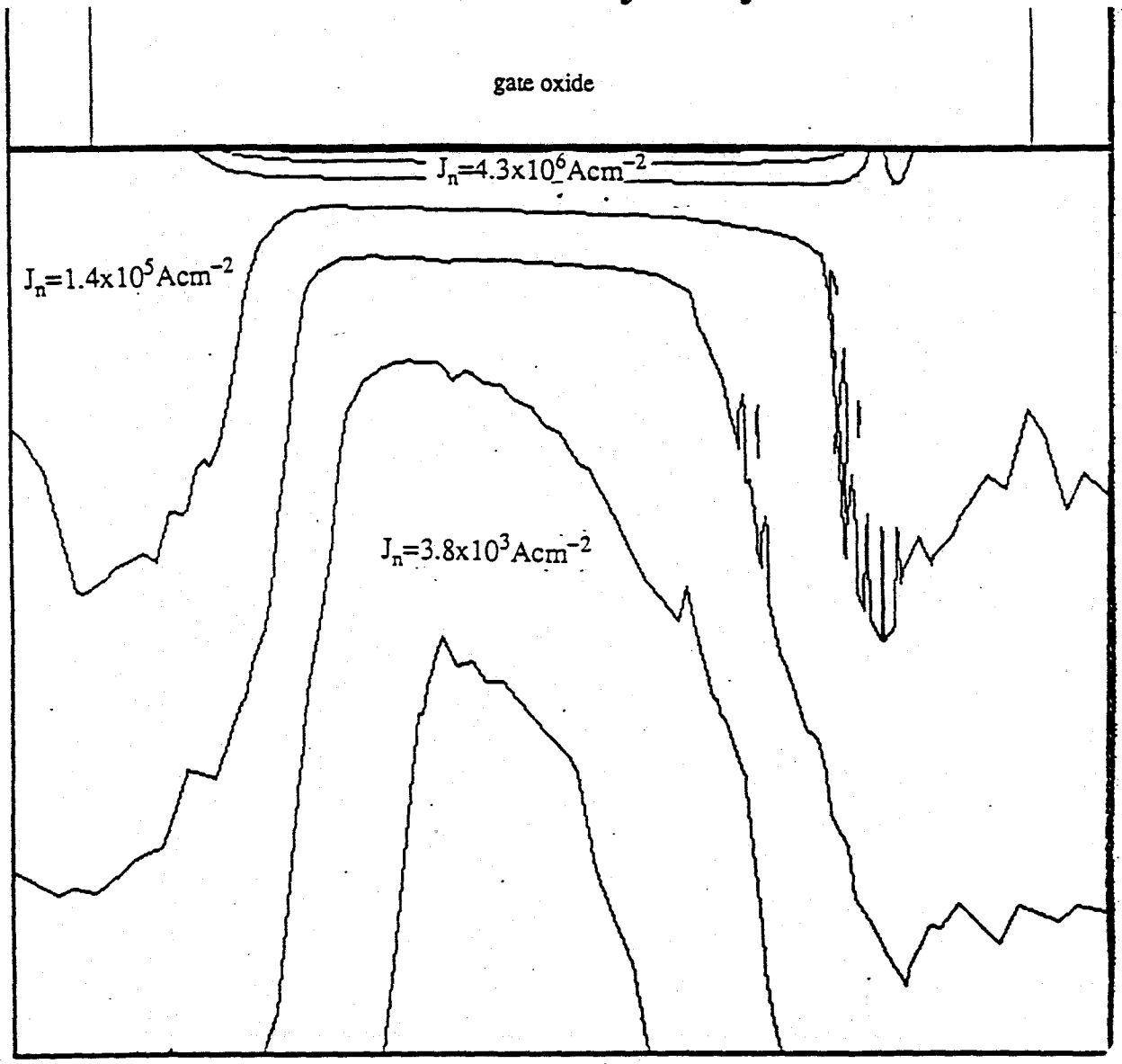

from Roberts, Modelling and Simulation of Small Geometry Silicon Devices, University of Waterloo

Current density, drift-diffusion model

Simulation Results
Two-Dimensional Hydrodynamic

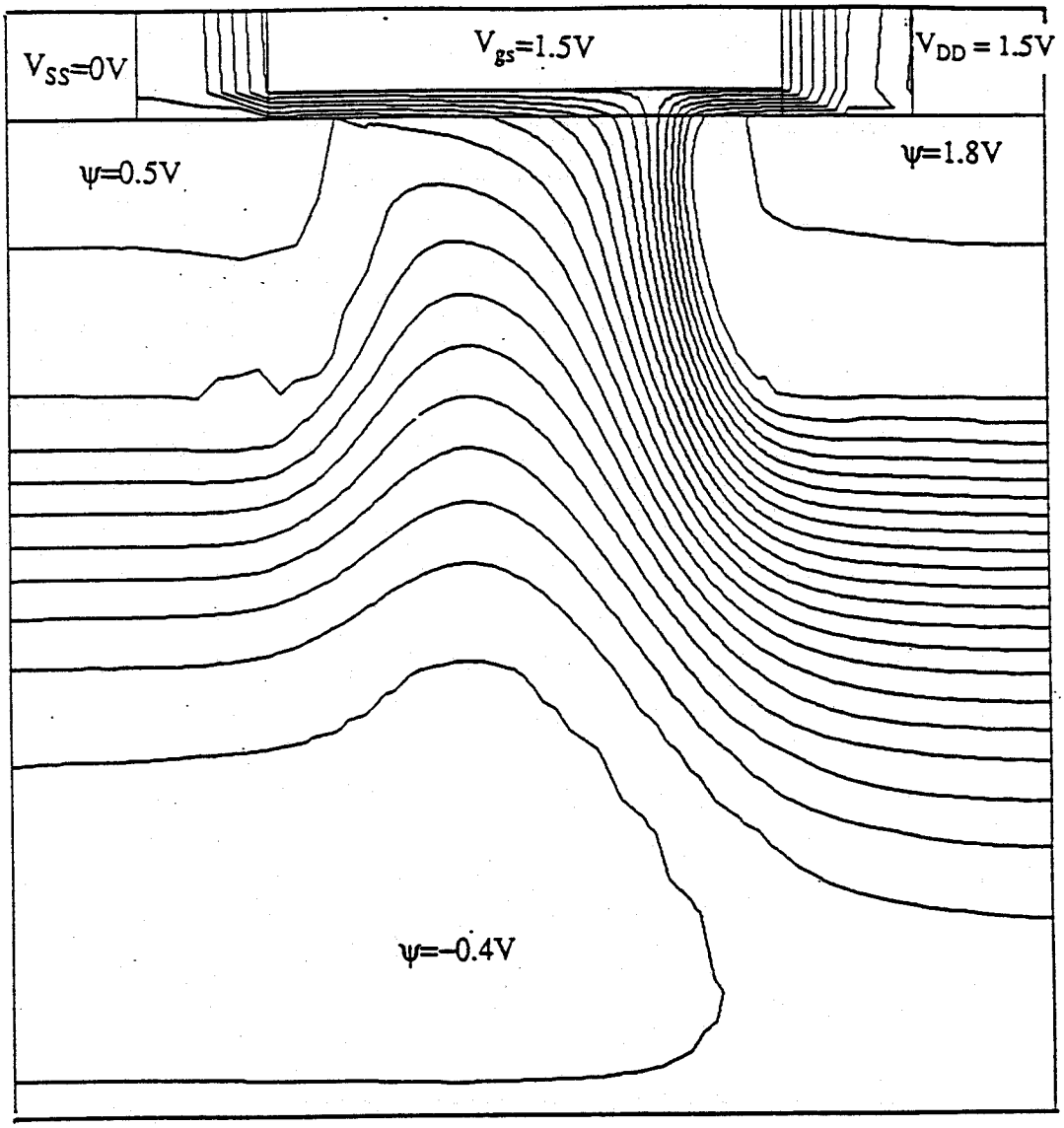

from Roberts, Modelling and Simulation of Small Geometry Silicon Devices, University of Waterloo

Potential contour plot, saturation, hydrodynamic model

Simulation Results
Two-Dimensional Hydrodynamic

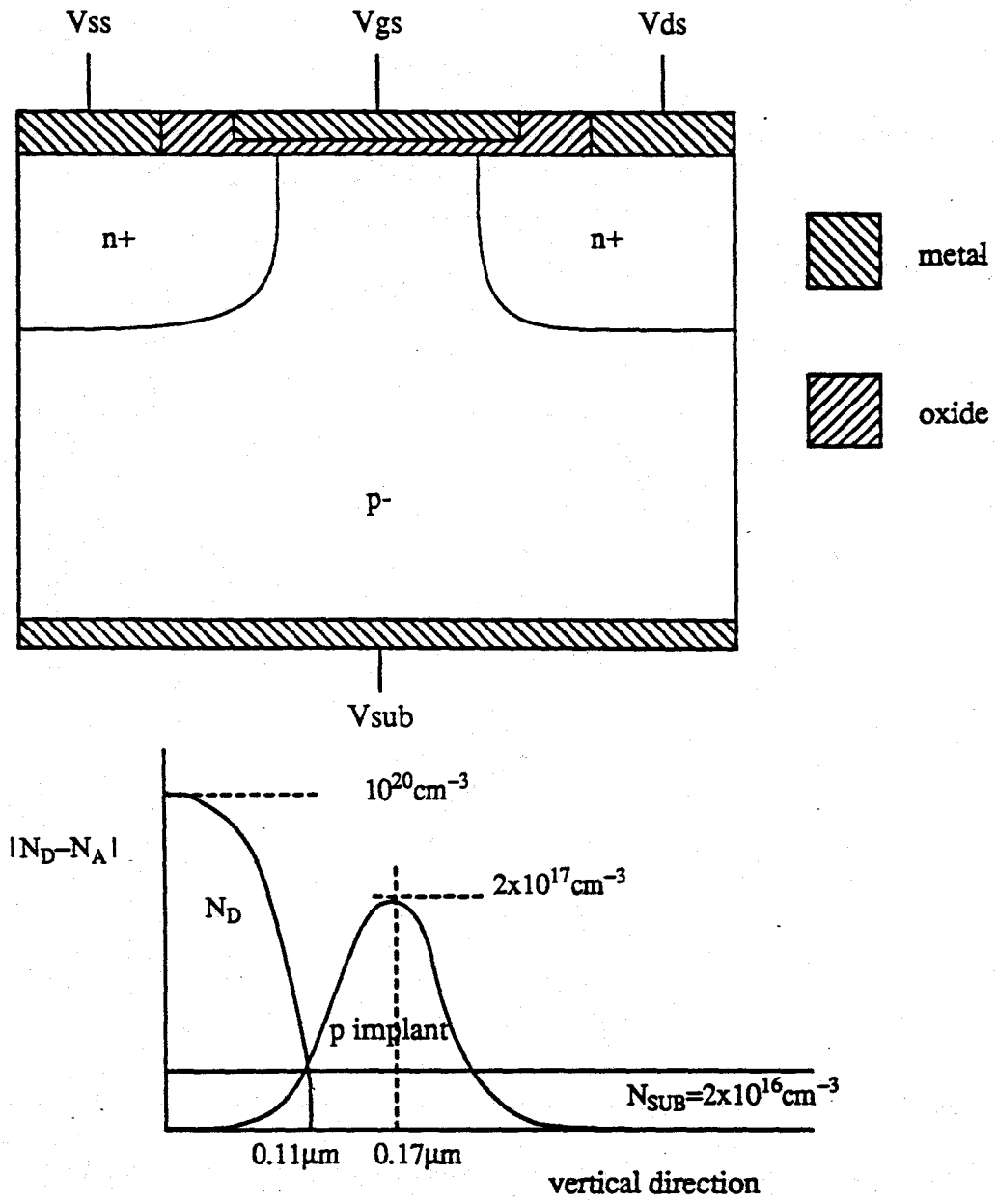

from Roberts, Modelling and Simulation of Small Geometry Silicon Devices, University of Waterloo

Layout of a 0.1 μm MOSFET

Simulation Results
Two-Dimensional Hydrodynamic

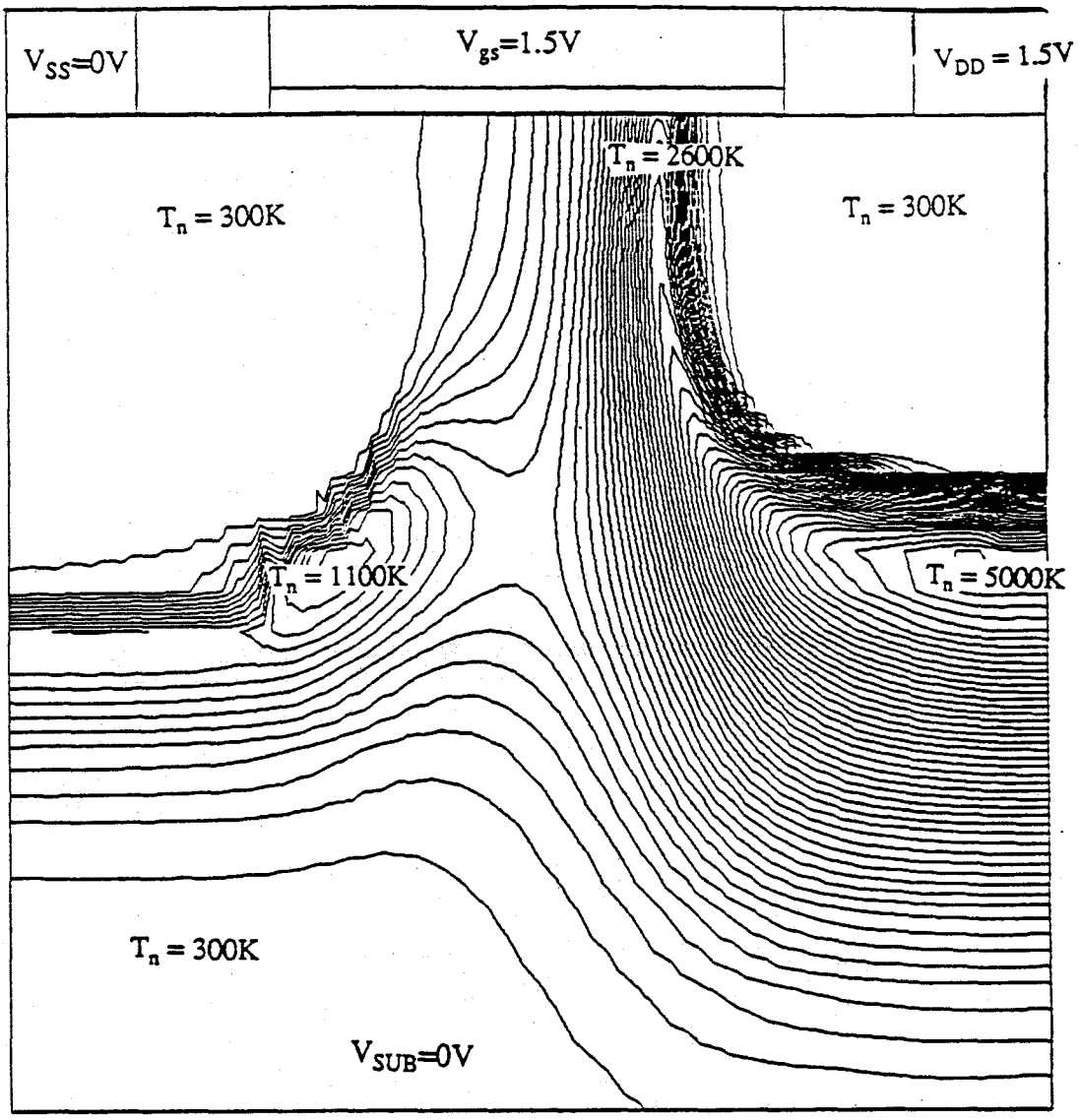

from Roberts, Modelling and Simulation of Small Geometry Silicon Devices, University of Waterloo

Electron temperature, hydrodynamic model

Simulation Results
Two-Dimensional Hydrodynamic

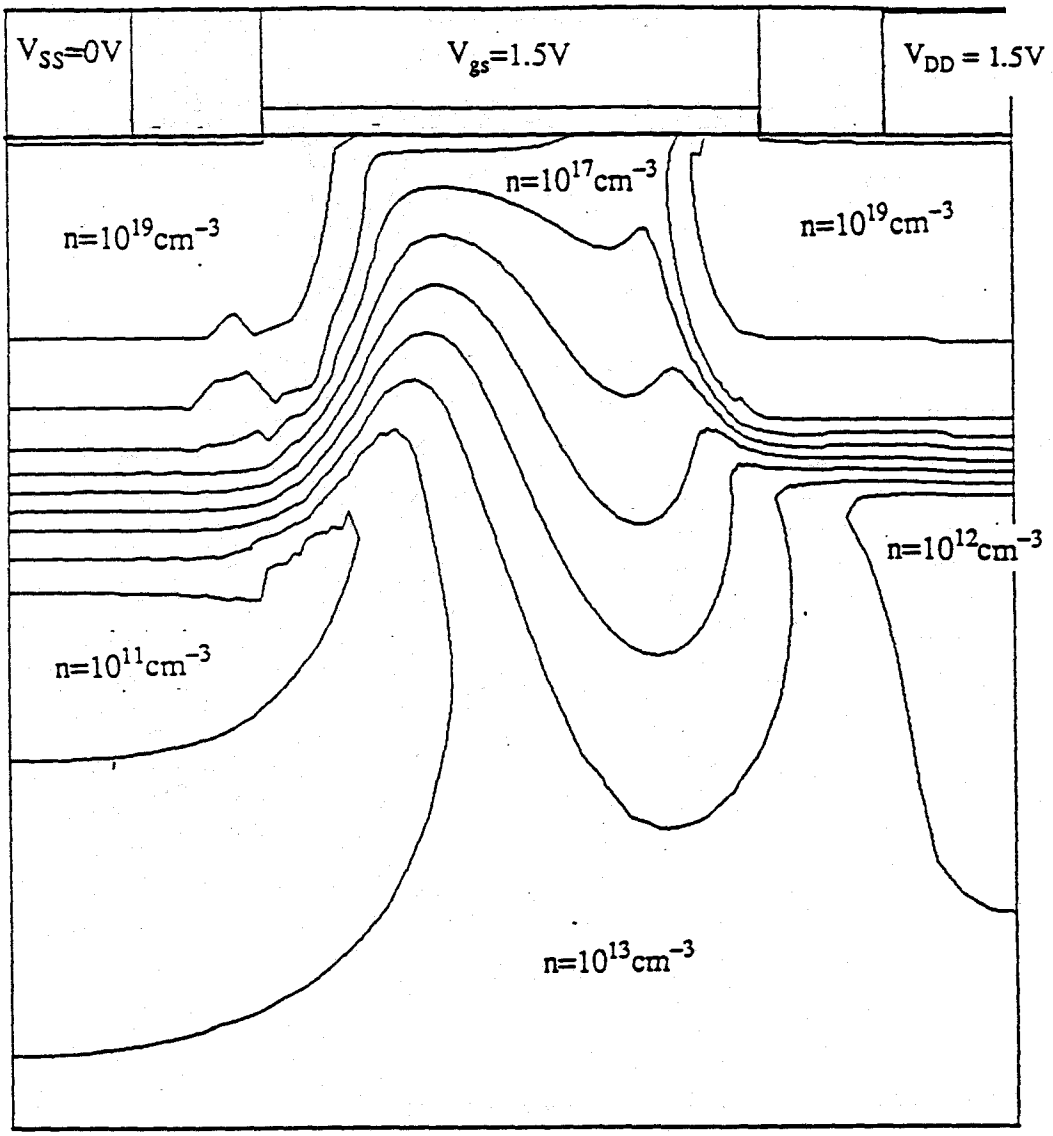

from Roberts, Modelling and Simulation of Small Geometry Silicon Devices, University of Waterloo

Electron concentration, hydrodynamic model

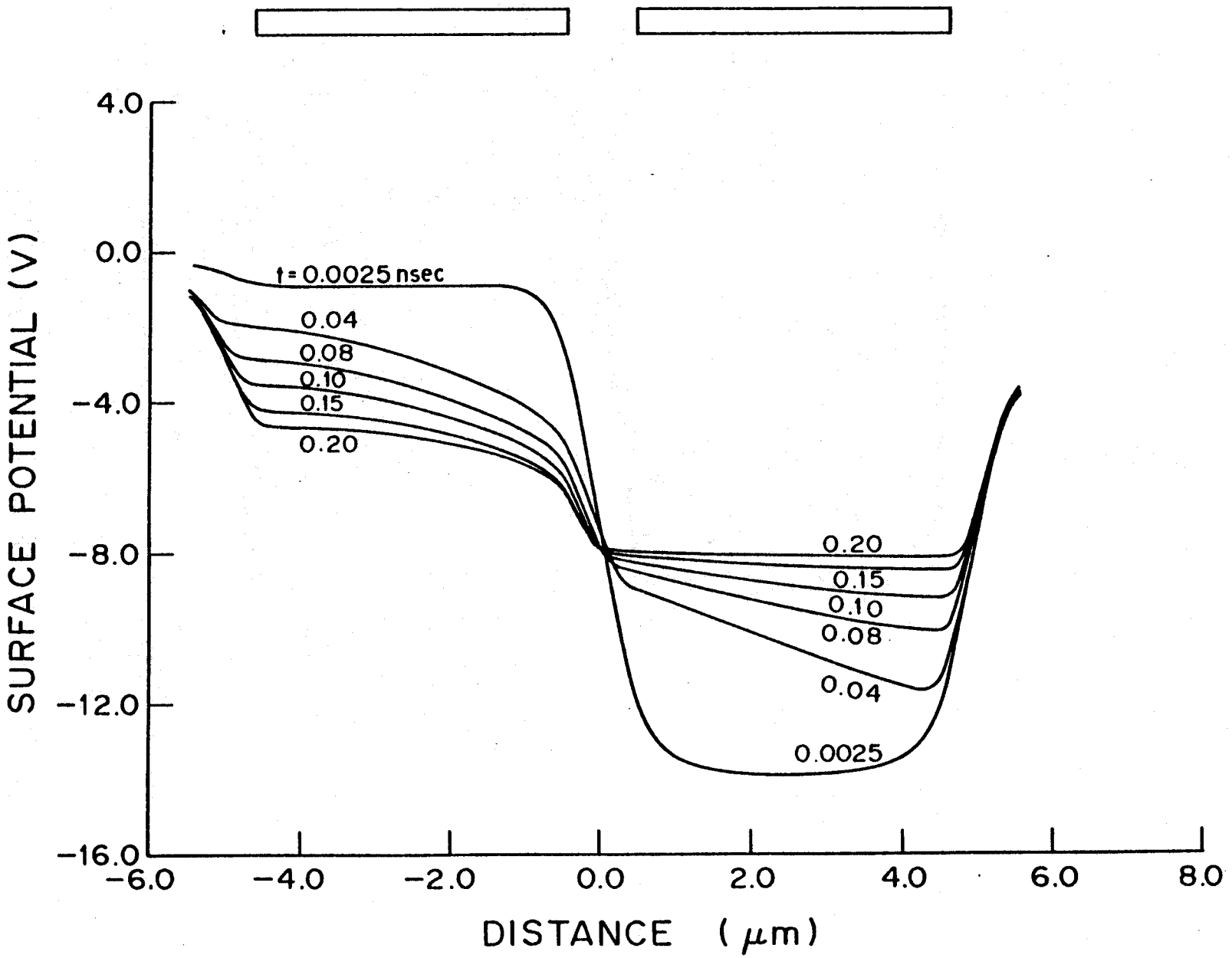
4.0
0.0
-4.0
-8.0
-12.0
-16.0
SURFACE POTENTIAL (V)
t = 0.0025 nsec
0.04
0.08
0.10
0.15
0.20
0.20
0.15
0.10
0.08
0.04
0.0025
-6.0
-4.0
-2.0
0.0
2.0
4.0
6.0
8.0
DISTANCE (μm)

Simulation Results
Two-Dimensional Drift-Diffusion

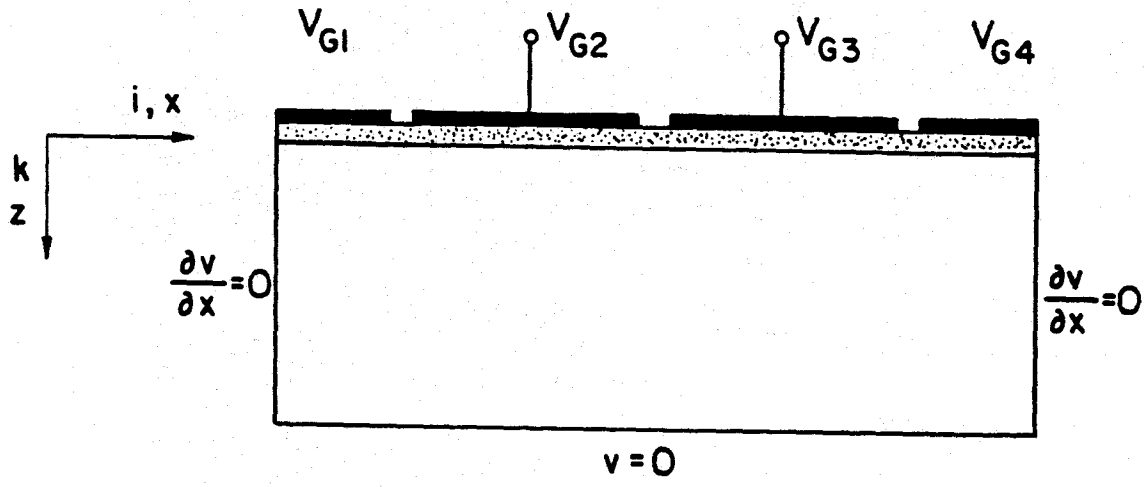

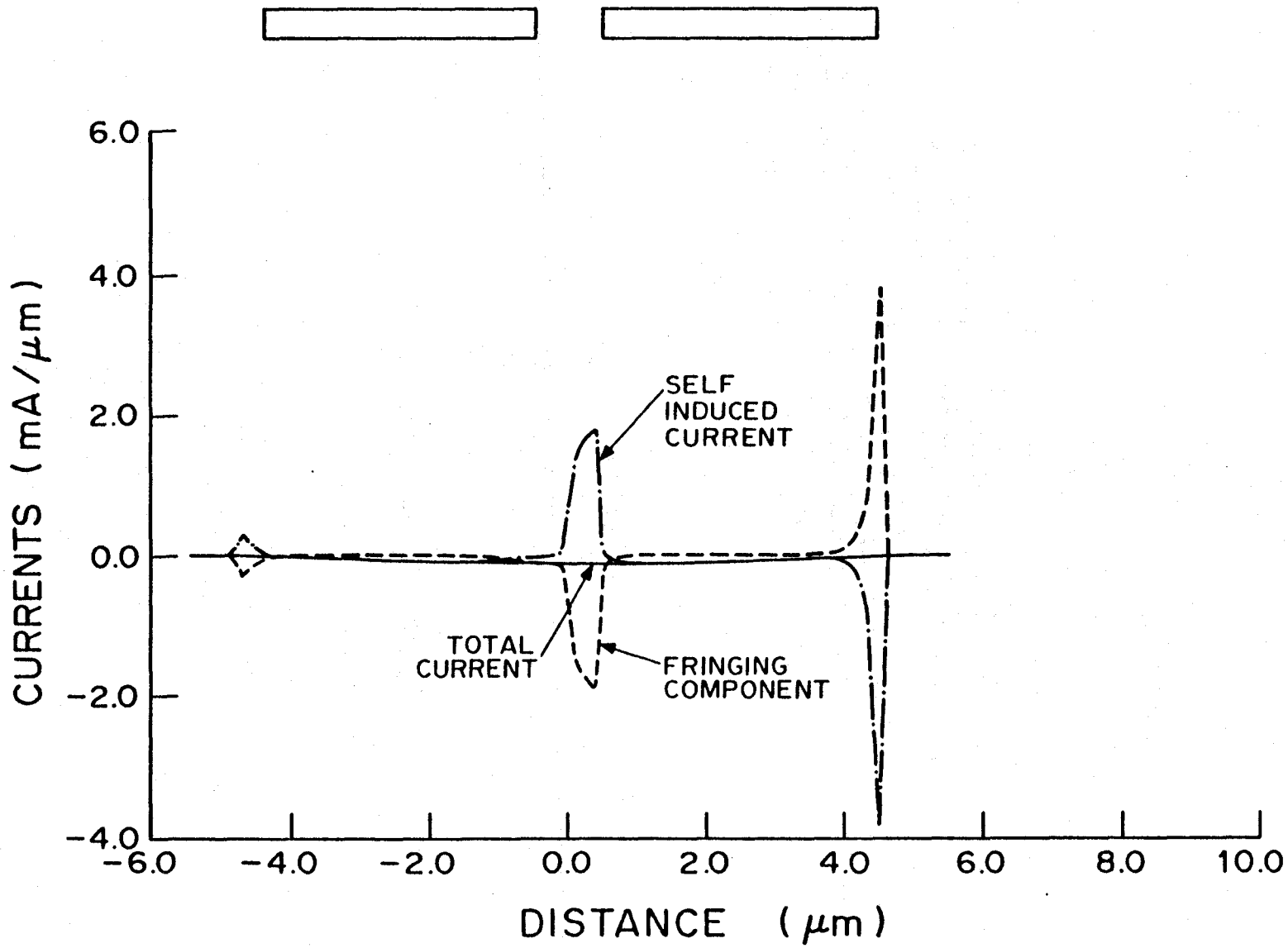
6.0
4.0
2.0
0.0
-2.0
-4.0
CURRENTS (mA/μm)
SELF
INDUCED
CURRENT
TOTAL
CURRENT
FRINGING
COMPONENT
-6.0
-4.0
-2.0
0.0
2.0
4.0
6.0
8.0
10.0
DISTANCE (μm)

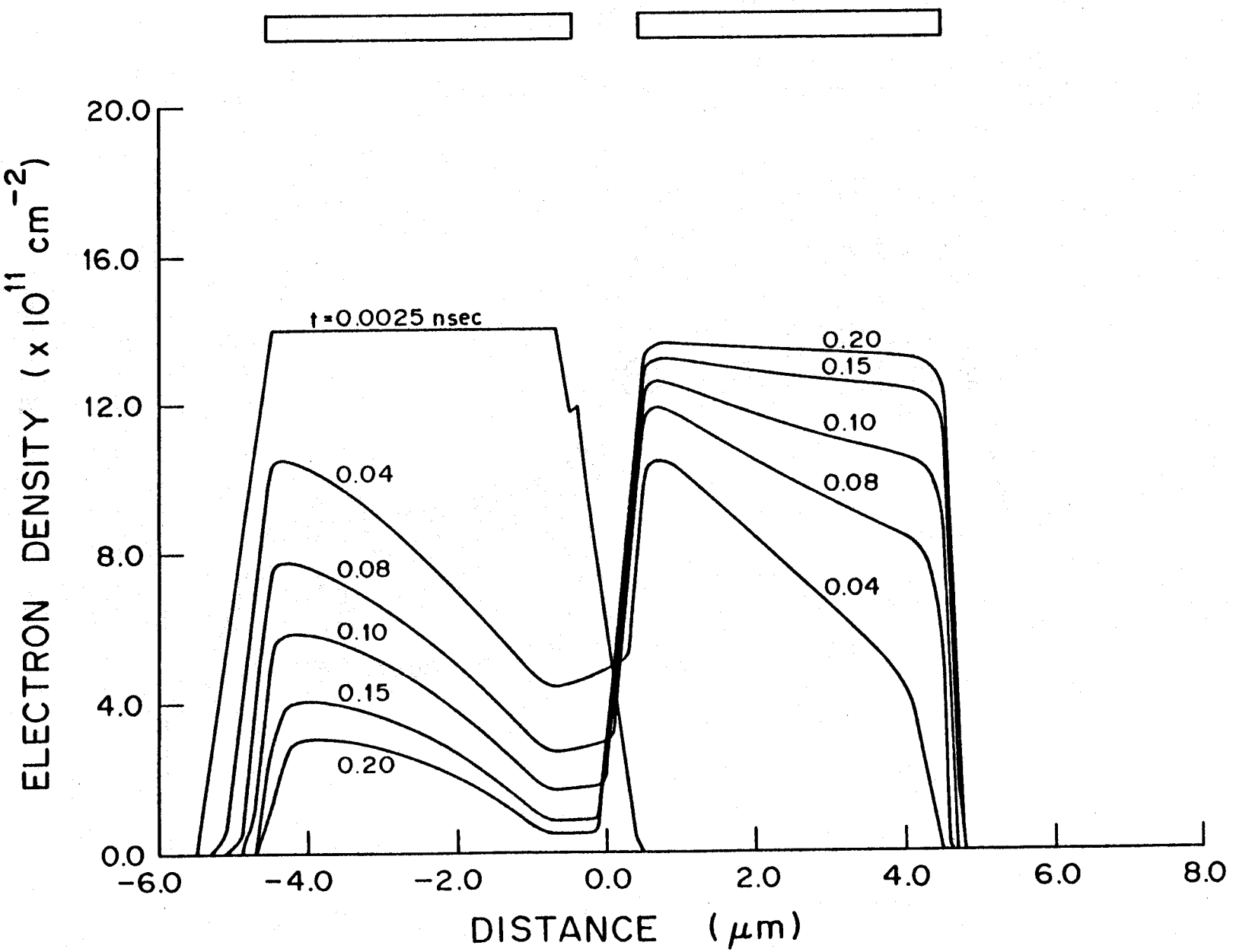
20.0
16.0
12.0
8.0
4.0
0.0
ELECTRON DENSITY (x 10^11 cm^-2)
t=0.0025 nsec
0.04
0.08
0.10
0.15
0.20
0.20
0.15
0.10
0.08
0.04
-6.0
-4.0
-2.0
0.0
2.0
4.0
6.0
8.0
DISTANCE (μm)

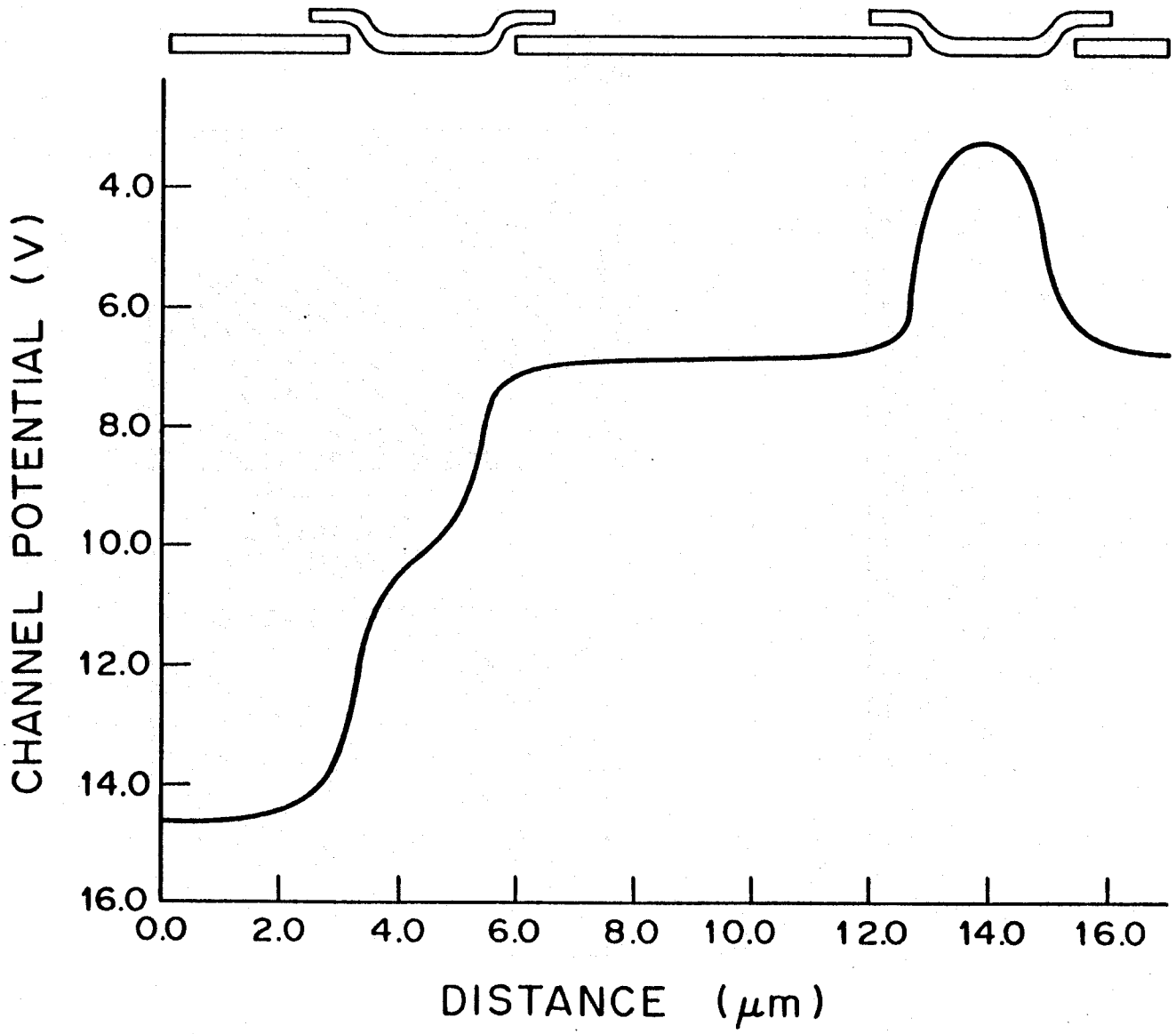
CHANNEL POTENTIAL (V)
4.0
6.0
8.0
10.0
12.0
14.0
16.0
0.0
2.0
4.0
6.0
8.0
10.0
12.0
14.0
16.0
DISTANCE (μm)

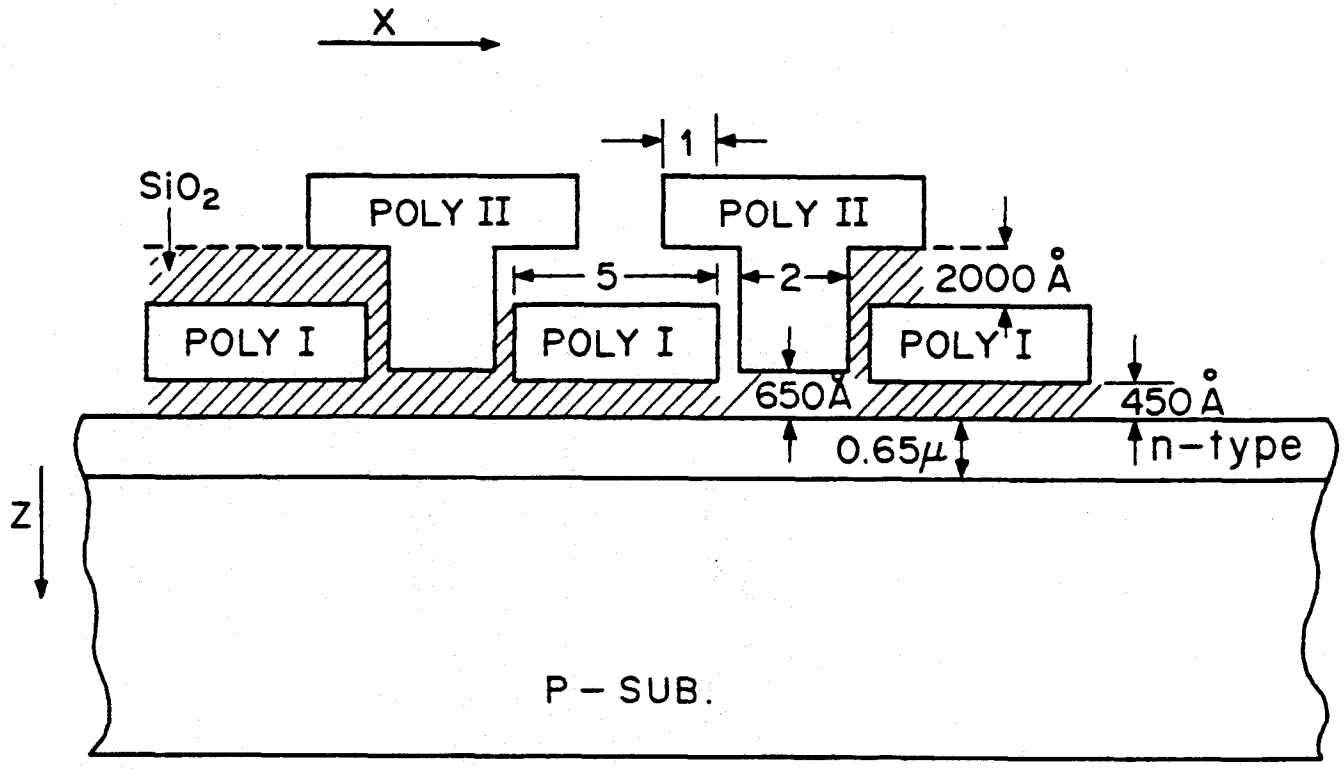

- DIMENSIONS IN μm OR AS SHOWN

Simulation Results
Three-Dimensional Drift-Diffusion

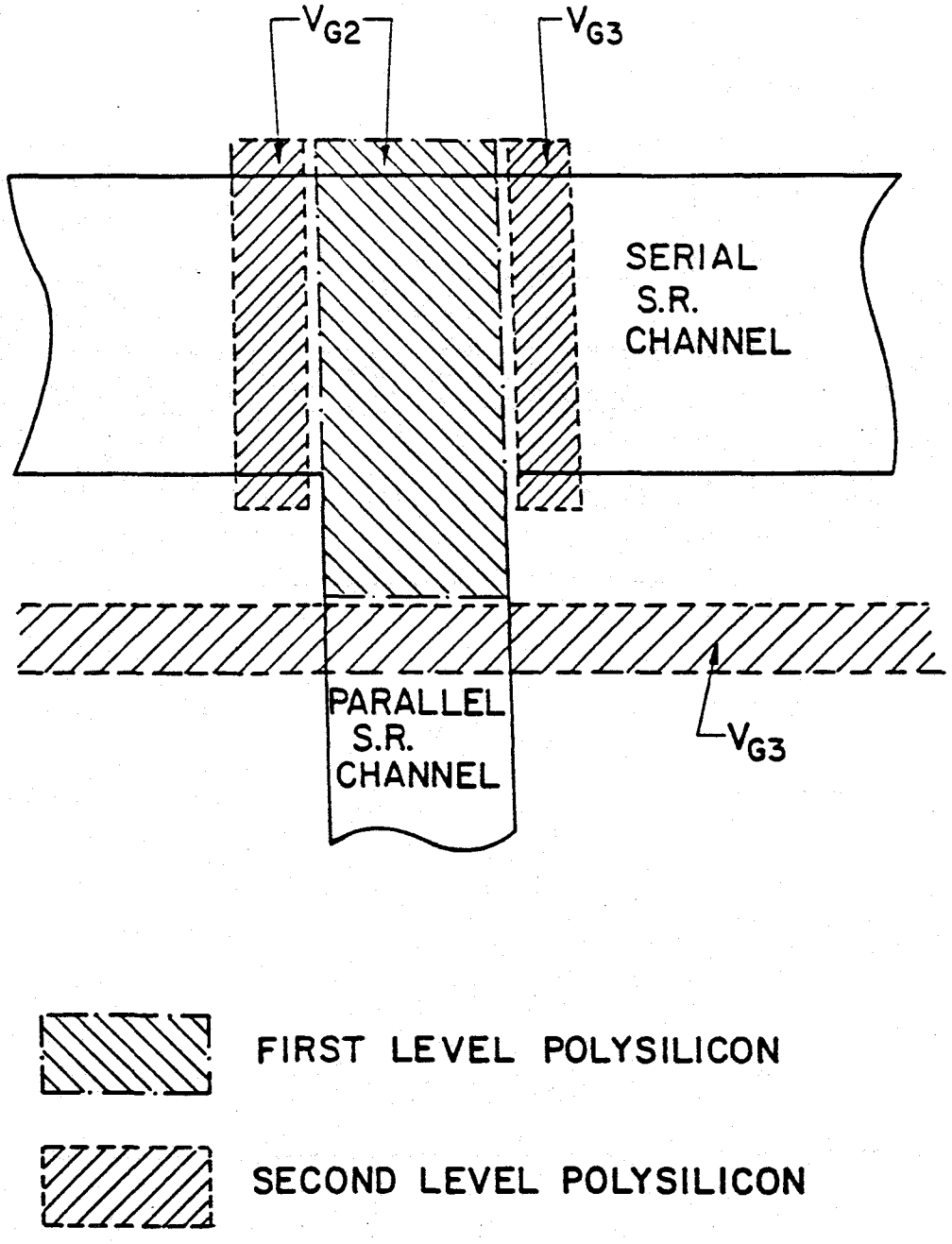

Serial-parallel shift register

Simulation Results
Three-Dimensional Drift-Diffusion

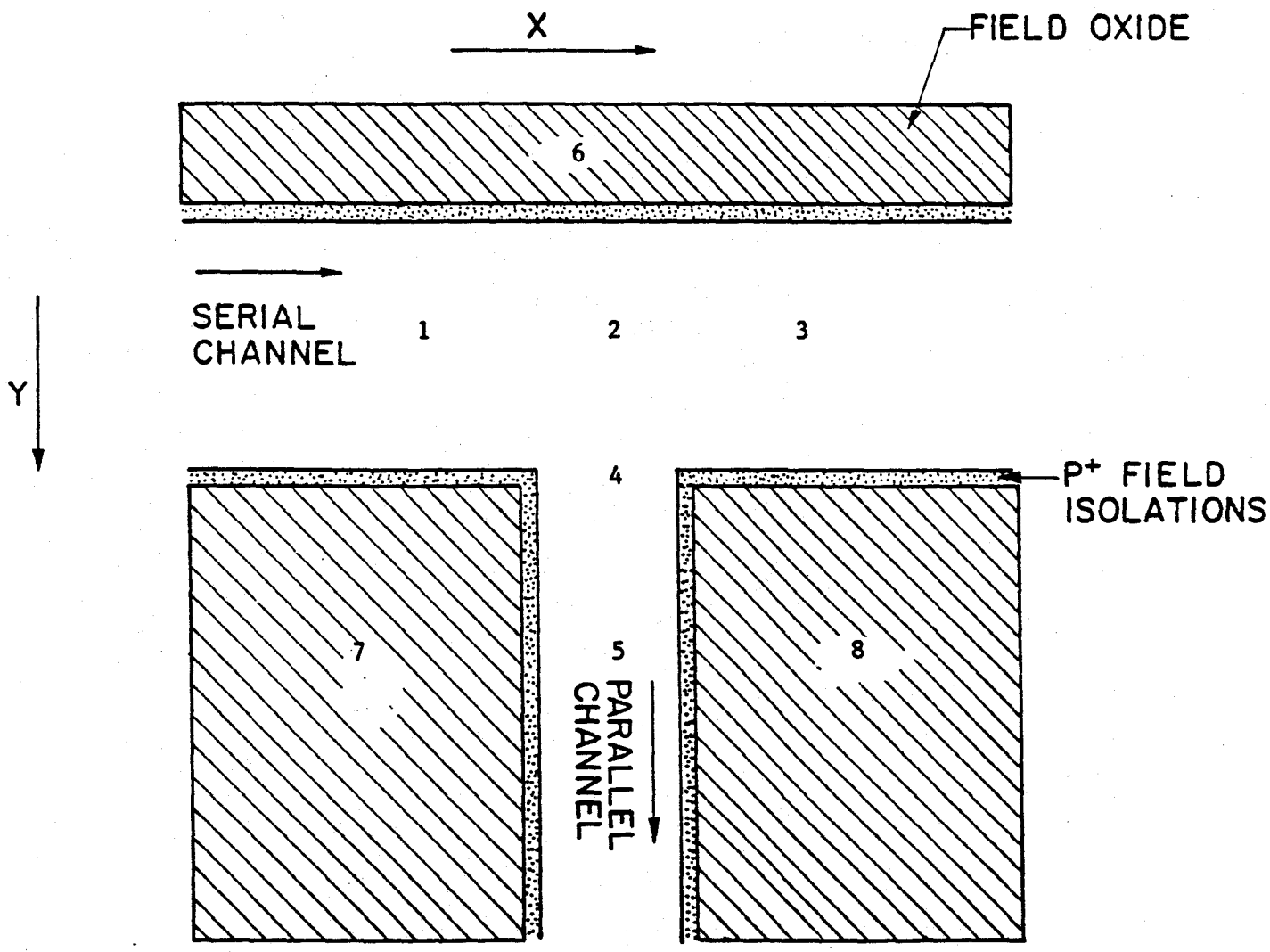

Serial-parallel shift register

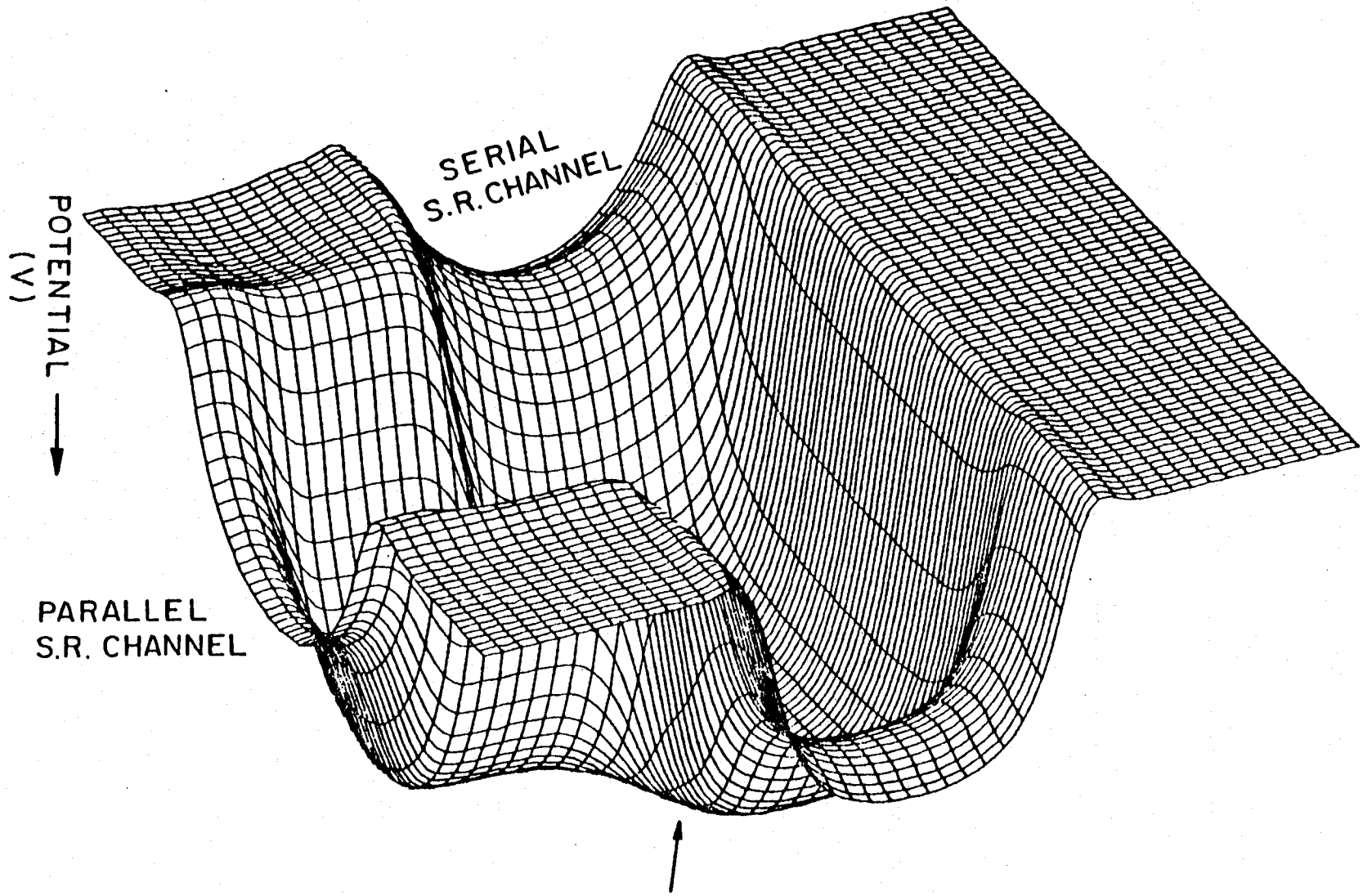
SERIAL
S.R.CHANNEL
POTENTIAL
(V)
PARALLEL
S.R. CHANNEL
Location of potential barrier

Simulation Results
Three-Dimensional Drift-Diffusion

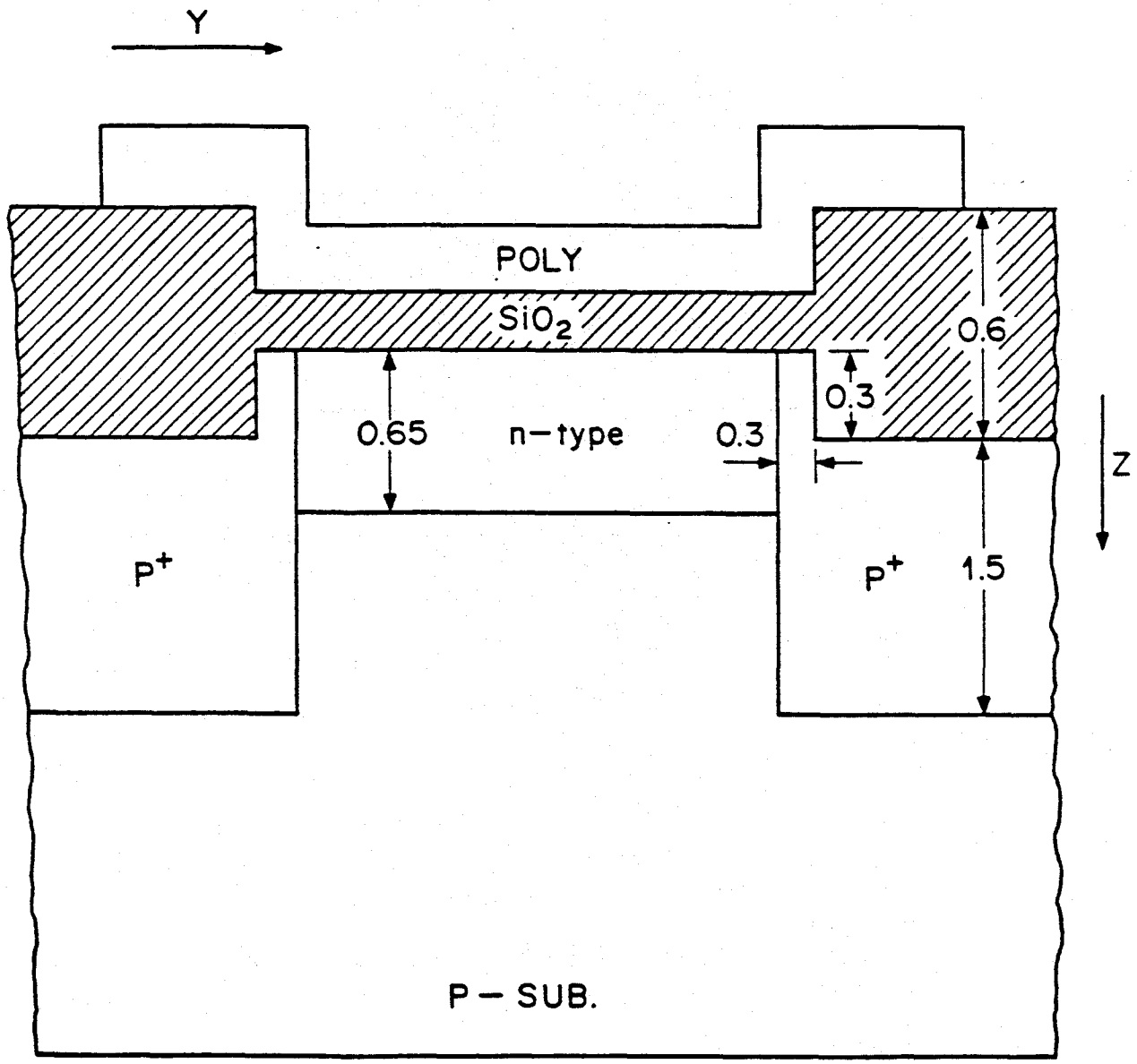

SPS channel width direction

Simulation Results
Three-Dimensional Drift-Diffusion

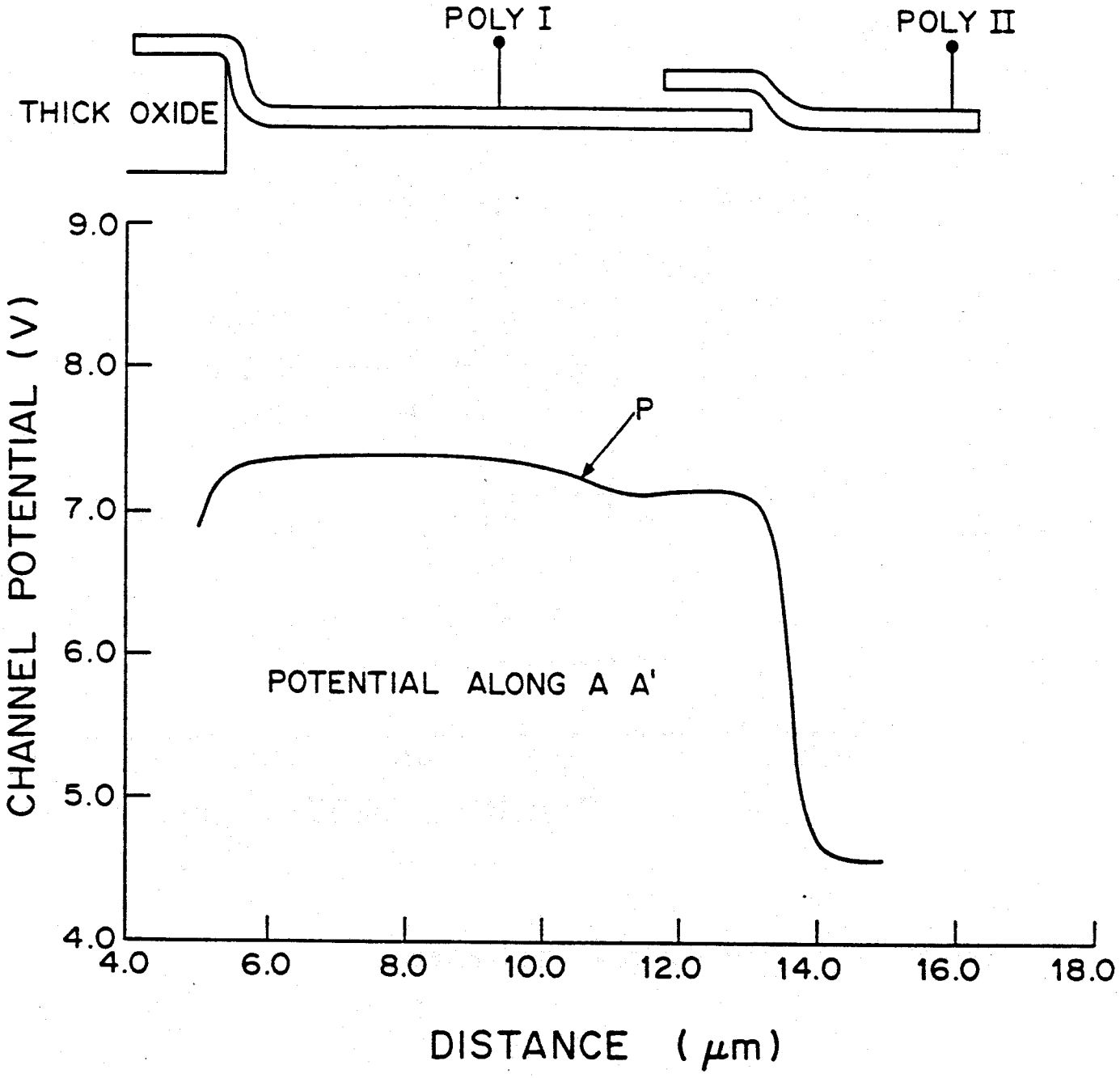

Location of potential barrier

Simulation Results
Three-Dimensional Drift-Diffusion

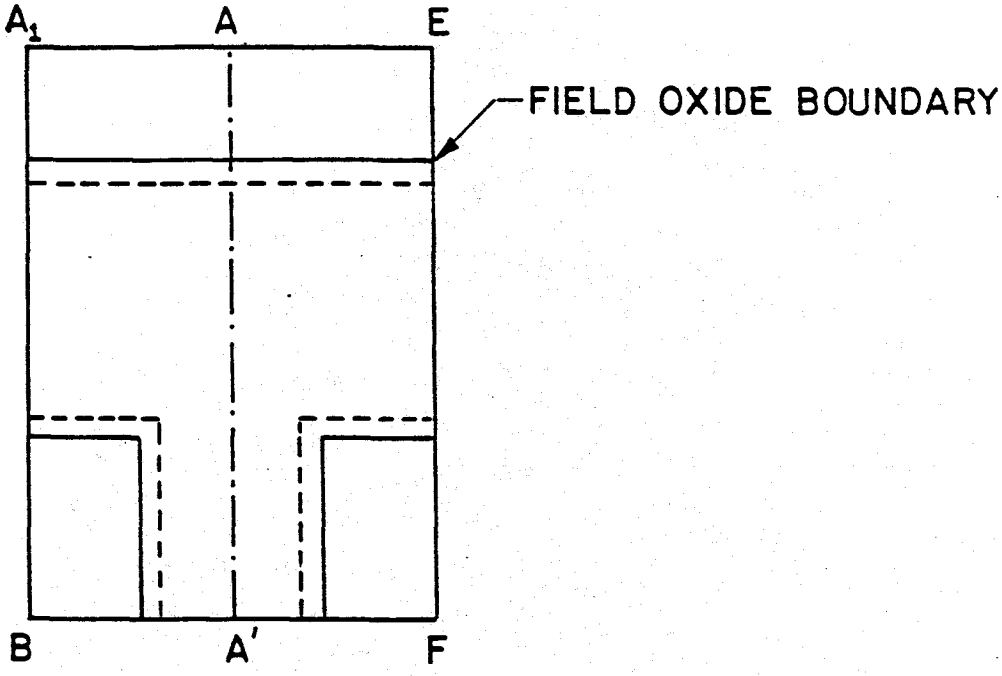

SPS Plan view

Interpretation of Results

All simulators lie

- some are sneakier than others

Typical lies:

- non-physical or near non-physical solutions
- incorrect grid refinement
- poor devices physics
- numerical noise
- garbage in, garbage out
- bugs

Always demend a physical expanation for results

Simulation Results
Three-Dimensional Drift-Diffusion

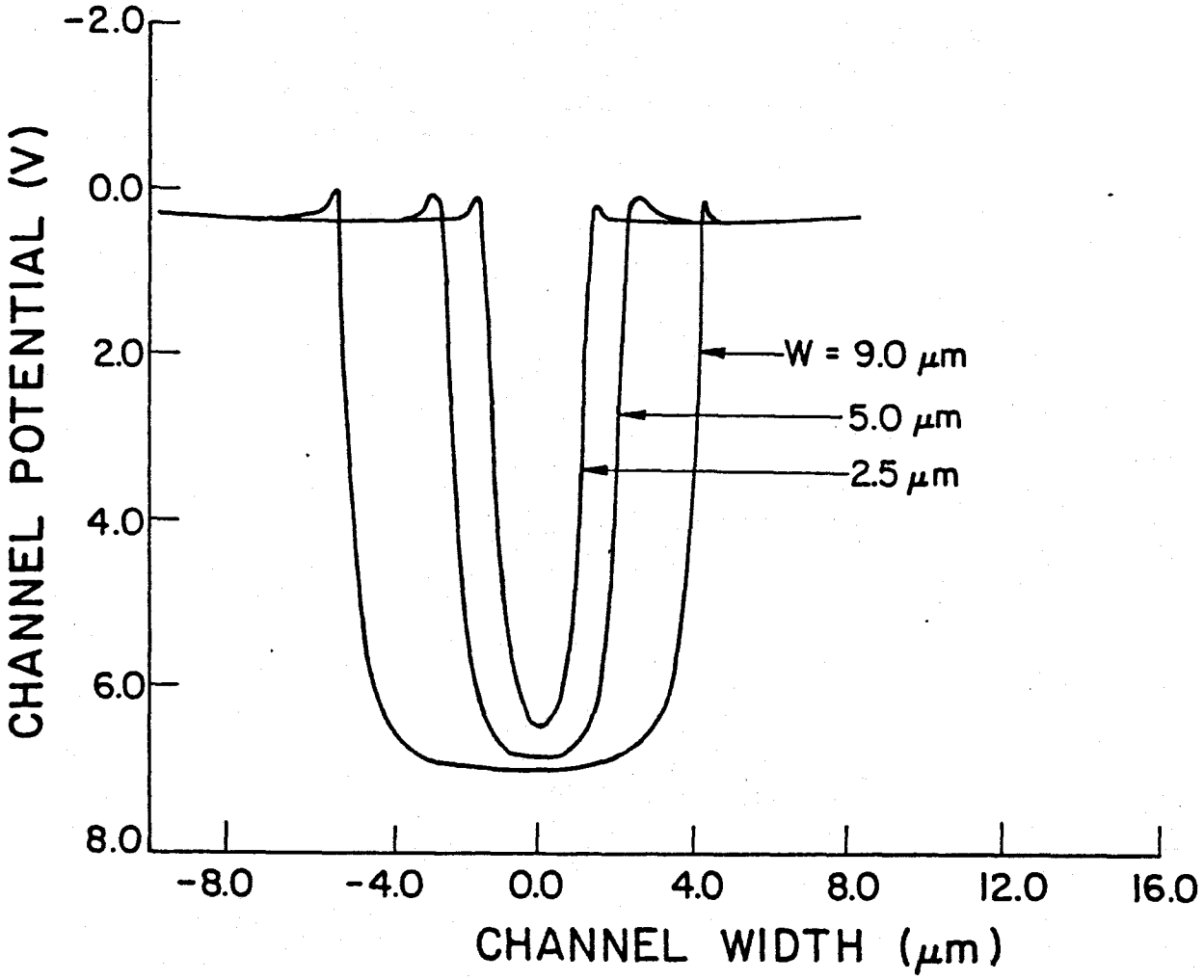

Barrier is due to the narrow width effect

[43] D.B. Scott and S.G. Chamberlain, "Experimental Confirmation of an Analytical Model for Charge Transfer in Charge-Couple Devices", *IEEE Journal of Solid State Circuits*, vol. SC-12, pp. 1-15, 1977.

[44] R.C. Kumar, D.J. Roulston, and S.G. Chamberlain, "A Study of the Effect of Peripheral Injection in Bipolar Transistors Using Simplified Computer Analysis", *IEEE Trans. Electron Devices*, vol. ED-24, pp. 1-12, March 1977.

[45] S.G. Chamberlain, B.Y. Woo, and D.B. Scott, "Modeling of Electrical Charge Injection into Charge-Coupled Devices", *Phys. Status Solidi (a)*, vol. 34, pp. 263-275, 1976.

[46] M.H. Elsaid, S.G. Chamberlain, and L.A.K. Watt, "Computer Model and Charge Transport Studies in Short Gate Charge-Coupled Devices", *Solid-State Electronics*, vol. 20, pp. 61-69, December 1977.

[47] S.G. Chamberlain and B.Y. Woo, "Transient Analysis of Electrical Charge Injection into Charge-Coupled Devices", *Int. J. Electronics*, vol. 40, pp. pp.569-586, 1976.

[48] C.H. Chan and S.G. Chamberlain, "Numerical Methods for Charge Transfer Analysis of Charge-Coupled Devices", *Solid-State Electronics*, vol. 17, pp. 491-499, 1974.

[49] R.C. Varshney, D.J. Roulston, and S.G. Chamberlain, "Some Properties Concerning the a.c. Impedance of p-i-n and p-n-n+ Diodes", *Solid-State Electronics*, vol. 17, pp. 699-706, 1974.

[50] C.H. Chan and S.G. Chamberlain, "A CCD Serial to Parallel Shift Register", *IEEE Journal of Solid-State Circuits*, vol. SC-8, pp. 388-391, October 1973.

[51] R.W. Brown and S.G. Chamberlain, "Quantum Efficiency of a Silicon Gate Charge Coupled Imaging Array", *Physica Status Solidi*, vol. 20, pp. 657-685, December 1973.

[52] S.G. Chamberlain, M.A. Copeland, and A.A. Ibrahim, "Some General Experimental Studies on Charge Coupled Device Circuits", *International J. Electronics*, vol. 35, pp. 833-846, 1973.

[53] R.C. Varshney, D.J. Roulston, and S.G. Chamberlain, "Determination of neutral region carrier concentrations in p-n junctions using Quasi-Fermi levels", *International Journal of Electronics*, vol. 3, pp. 15-23, July 1973.

[54] J.C. Tandon, D.J. Roulston, and S.G. Chamberlain, "Reverse-bias characteristics of a P+-N-N+ Photodiode", *Solid State Electronics*, vol. 15, pp. 669-685, 1972.

[55] D.J. Roulston, S.G. Chamberlain, and J. Seghal, "Simplified Computer-Aided Analysis of Double-Diffused Transistors Including Two-Dimensional High Level Effects IEEE Trans. on Electron Devices", , vol. ED-19, no. 6, pp. 809-820, 1972.

[56] S.G. Chamberlain, "Photosensitivity and Scanning of Silicon Image Detector Arrays", *IEEE Journal of Solid State Circuits*, vol. SC-4, no. 6, pp. 333-343, 1969.

Related Papers Published in Refereed Journals

[1] R.J. Inkol, W.D. Washkurak, and S.G. Chamberlain, "A large dynamic range photodetector array for Acousto-Optic spectrum analyzers", *Submitted for publication*, pp. 1-14.

[2] M. J. Van der Tol and S. G. Chamberlain, "Drain-Induced Barrier-Lowering in Buried-Channel MOSFET's", *IEEE Journal of Solid-State Circuits*, pp. 1-15, Submitted for publication.

[3] S. H. Hood and S. G. Chamberlain, "Color Filter Arrays for Silicon Solid-State Image Array Sensors", *Accepted for publication Canadian Journal of Physics*, vol. 69, pp. 1-16, March/April 1991.

[4] J. W. Roberts, S. G. Chamberlain, and J.R.F. McMacken, "Energy-Momentum Transport Based Simulator Adapted to CHORD", *Accepted for Publication in Canadian Journal of Physics*, vol. 69, pp. 1-15, March/April 1991.

[5] J.R.F. McMacken and S.G. Chamberlain, "A Numerical Model for Two-Dimensional Transient Simulation of Amorphous Silicon Thin-Film Transistors", *IEEE Trans. on Computer-Aided Design of Integrated Circuits and Systems*, vol. Accepted for publication, pp. 1-14, 1991.

[6] M. J. Van der Tol and S. G. Chamberlain, "Buried-Channel MOSFET Model for SPICE", *IEEE Trans. on Computer-Aided Design of Integrated Circuits and Systems*, vol. 10, pp. 1-15, July 1991.

[7] C. R. Smith and S. G. Chamberlain, "Theory and design Methodology for an Optimum Single-Phase CCD", *IEEE Trans on Electron Devices*, pp. 1-14, Accepted for publication 1991.

[8] W. D. Washkurak and S. G. Chamberlain, "High Speed CCD Image sensor for acousto-optic signal processing", *IEEE Transactions on Electron Devices*, pp. 1-15, Submitted for publication, July 1990.

[9] W. D. Washkurak and S. G. Chamberlain, "Wide Dynamic range CCD Area Image Sensors", *IEEE Trans on Electron Devices*, pp. 1-14, Submitted for publication, August 1990.

[10] S. G. Chamberlain and W. D. Washkurak, "High speed low noise Time-Delay-and-Integration Imager", *IEEE Trans on Electron Devices*, pp. 1-16, Submitted for publication, August 1990.

[11] J.R.F. McMacken and S. G. Chamberlain, "Analytic and Iterative Transit Time Models for VLSI MOSFET's in strong inversion", *IEEE Journal of Solid-State Circuits*, vol. 25, pp. 1257-1267, No 5, October 1990.

[12] J. W. Roberts and S. G. Chamberlain, "Energy-Momentum Transport Model for Small Geometry Silicon Device Simulation", *COMPEL, Inter. Journal for Computation and Mathematics in Electrical and Electronic Engineering*, vol. 9, no. 1, pp. 1-22, March 1990.

[13] J.W. Roberts and S. G. Chamberlain, "A CMOS model for computer aided circuit analysis and design", *IEEE J. Solid-State Circuits*, vol. 24, no. 1, pp. 128-138, 1989.

[29] M.H. El-Diwany, D.J. Roulston, and S.G. Chamberlain, "Design of Low-Noise Bipolar Trans-impedance Preamplifiers for Optical Receivers", *IEE Proc.*, vol. 128, Pt. G., no. 6, pp. 299-306, 1981.

[30] R. Kumar, D.J. Roulston, and S.G. Chamberlain, "Two-Dimensional Simulation of a High-Voltage p-i-n Diode with overhanging Metalization", *IEEE, Trans. on Electron Devices*, vol. ED-28, no. 5, pp. 534-540, 1981.

[31] R. Kumar, S.G. Chamberlain, and D.J. Roulston, "An algorithm for two dimensional simulation of reverse-biased beveled p-n junction", *Solid-State Electronics*, vol. 24, pp. 309-311, 1981.

[32] R. Kumar, D.J. Roulston, and S.G. Chamberlain, "Accurate Two-Dimensional Simulation of Double-Beveled p-n Junctions", *Solid-State Electronics*, vol. 24, pp. 377-379, 1981.

[33] H.S.A. Zohdy, S.G. Chamberlain, and L.A.K. Watt, "Limitations of Multilevel Storage in Charge-Coupled Devices", *IEEE Trans. on Electron Devices*, vol. ED-27, pp. 1559-1575, September 1980.

[34] S.G. Chamberlain, "Advances in CCD Scanners with On-Chip Signal Processing for Electronic Imaging", *The Radio and Electronic Engineer*, vol. 50, pp. 249-257, May 1980.

[35] D.B. Scott and S.G. Chamberlain, "Modeling and Experimental Simulation of the Low-Frequency Transfer Inefficiency in Bucket-Brigade Devices", *IEEE Trans. on Electron Devices*, vol. ED-27, pp. 405-414, February 1980.

[36] R.J. Inkol and S.G. Chamberlain, "Design and Realization of a Two-Level 64k byte CCD Memory System for Microcomputer Applications", *IEEE Journal of Solid-State Circuits*, vol. SC-15, pp. 131-135, February 1980.

[37] S.G. Chamberlain, "New Profiled Silicon Photodetector for Improved Short-Wavelength Quantum Efficiency", *Journal of Applied Physics*, vol. 50, pp. 7228-7232, November 1979.

[38] D.B. Scott and S.G. Chamberlain, "A Calibrated Model for the Subthreshold Operation of Short Channel MOSFET Including Surface States", *IEEE Journal of Solid-State Circuits*, vol. SC-14, pp. 633-644, June 1979.

[39] S.G. Chamberlain, D.J. Roulston, and S.P. Desai, "Spectral Response Limitation Mechanisms of a Shallow Junction n+-p Photodiode", *IEEE Trans. Electron Devices*, vol. ED-25, pp. 241-246, February 1978.

[40] S.G. Chamberlain and D.H. Harper, "MTF Simulation Including Transmittance Effects and Experimental Results of Charge Coupled Imagers", *IEEE Journal of Solid-State Circuits*, vol. SC-13, pp. 71-80, February 1978.

[41] J.M. White and S.G. Chamberlain, "A Multiple-Gate CCD Photodiode Sensor Element for Imaging Arrays", *IEEE Trans. Electron Devices*, vol. ED-25, pp. 125-131, 1978.

[42] M.H. Elsaid and S.G. Chamberlain, "Short-Channel Effects on the Input Stage of Surface-Channel CCD's", *IEEE Trans. on Electron Devices*, vol. ED-24, pp. 1164-1171, September 1977.